PPM Annual Report 2015

The Annual Report for the PPM Research Centre

DEPARTMENT OF GEOLOGY

UNIVERSITY OF JOHANNESBURG

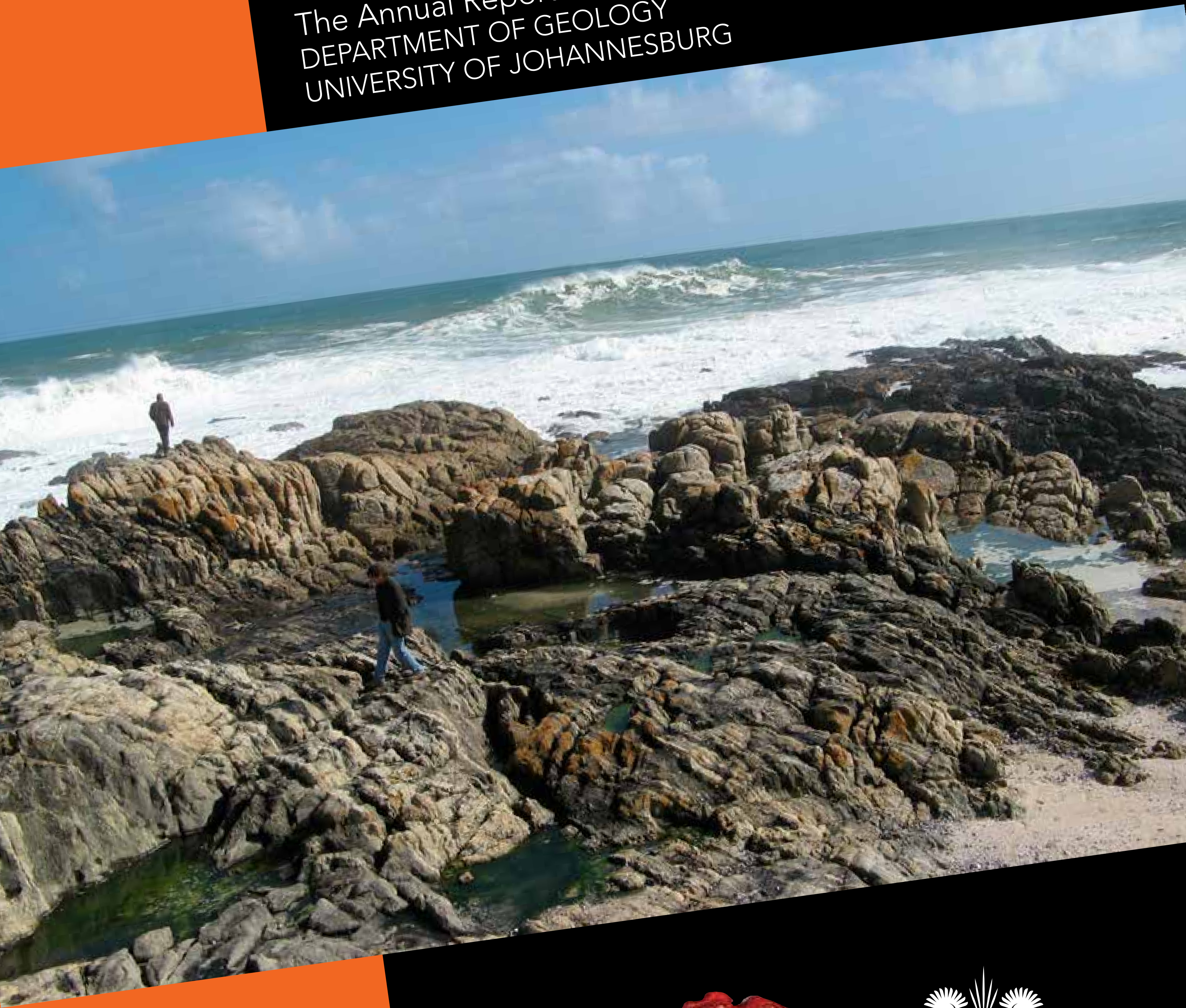

PPM

UNIVERSITY OF JOHANNESBURG

The Annual Report of the PPM Research Centre compiled by Jan Kramers.
Layout and design by UJ Graphic Studio

Special thanks/Acknowledgements
We wish to extend a special word of thanks to all our corporate and governmental financial and logistical supporters (in alphabetical order):
African Rainbow Minerals
Anglo American
Anglo Coal
Anglo Gold Ashanti
Anglo Platinum
Anglo Research
Assmang
Assore
Coaltech
Cradle of Humankind Trust
Department of Science and Technology (DST)
Deutsche Akademische Austauschdienst (DAAD)
Lonmin
National Research Foundation (NRF)
Nkomati Joint Venture
Rand Uranium (Gold One)
Two Rivers Platinum Mine
Vale

Please direct all enquiries and proposals for research to:
Prof. Jan Kramers or Prof. Fanus Viljoen
PPM, Department of Geology
University of Johannesburg
Auckland Park Kingsway Campus
PO Box 524, Auckland Park 2006
Johannesburg, South Africa
E-mail: jkramers@uj.ac.za or fanusv@uj.ac.za
Tel: +27(0)11 559 4701
Fax: +27(0)11 559 4702

Cover photo: the Sea point outcrop visited by Darwin in 1836 and the subject of much philosophizing about granite emplacement ever since. The late Proterozoic Malmesbury Group is intruded by the Cape Granite in a complex interfingering mode with large K-feldspars ('dents de cheval' or horses' teeth) appearing in the intruded metasediments. The picture is to remind us that field geology is always where it starts, no matter what analytical sophistication is applied. Photo J. Kramers

Header photo: the flight tube of the Nu Instruments Plasma II MC-ICP-MS at the UJ Geology Department. Photo J. Kramers

Footer photo: Joburg Skyline from the Geology Department. Photo J. Kramers

INTRODUCTION

The year 2015 has been one of consolidation of the PPM Centre and its new coexistence with the DST-NRF Centre of Excellence for integrated Mineral and Energy Resource Analysis (CIMERA). The division of roles is clear: one is a Research Centre within the framework of the University of Johannesburg, funded by its University Research Council, while the other is an inter-university Centre of Excellence, funded nationally. A win-win situation developed. Two new senior academic posts pledged by UJ in connection with CIMERA were created, and as a result the Geology Department, and PPM, could welcome two new Staff members in 2015: Prof Sebastian Tappe, an expert on kimberlites and the Earth's mantle, and Dr Jérémie Lehmann, a structural geologist with extensive experience in the Pan African orogenic belts, who both also already contributed to the PPM brand. Nevertheless, in order not to be a shadow of the larger CIMERA Centre, PPM has had to heed the call by UJ to some extent, to *reinvent itself*: taking advantage not only of the UJ culture in this regard, but also of the fact that URC funded Research Centres have somewhat greater freedom of movement than the larger DST-NRF funded ones. In this sense the diversification into areas of research not originally the core focus of PPM (Paleoproterozoic Mineralization) is continuing, encompassing coal petrography, the study of mobile belts, environmental and medical geology, and work related to hominin evolution. An enormous boost to research in all these fields will be the establishment of the new laser ablation MC-ICP-MS laboratory, with the Nu Instruments Plasma II instrument having been delivered, assembled and successfully tested in October-November 2015.

ORGANIGRAM OF THE PPM RESEARCH CENTRE 2015

UNIVERSITY OF JOHANNESBURG

Technical support Staff in PPM
Mr T. Ramaliba
Mr H. Gugwana

Academic Staff in PPM
Dr. G. Belyanin
Prof. Nic Beukes*
Mrs. Lauren Blignaut
Prof. Bruce Cairncross
Dr. Michiel de Kock
Prof. Marlina Elburg
Prof. Axel Hofmann
Mr. Mike Knoper
Prof. Jan Kramers*
Dr Jeremie Lehmann
Prof. Hassina Mouri
Mr. Freeman Senzani
Dr. Bertus Smith
Prof. Sebastian Tappe
Dr. Herman van Niekerk
Prof. Fanus Viljoen*
Dr. Clarisa Vorster
Prof. N. Wagner
(*leading PPM)

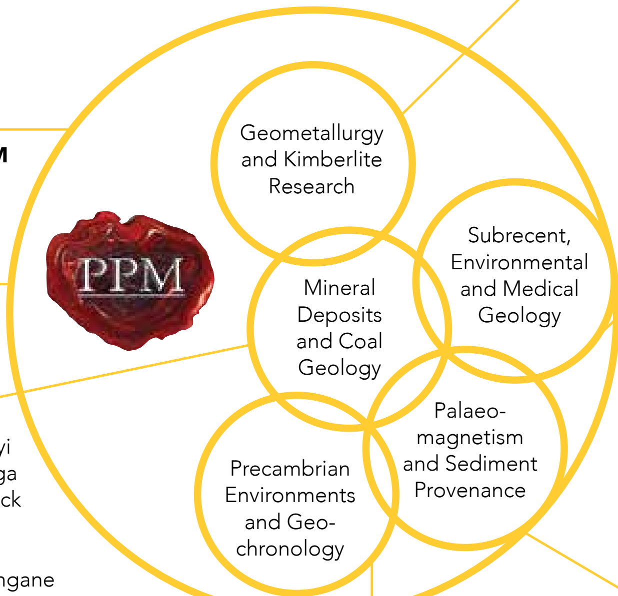

Dr A. Dongre
Mr. T. Dzvinamurungu
Ms. G. Mishra
Ms. B. Mkhize
Mr. E. Moitsi
Ms. B. Motloba
Ms. T. Mxinwa
Ms. T. Nkomo
Mr. C. Radzivhoni
Ms. N. Ramakoloi
Mr. D. Rose
Mr. A. McLoughlin

Mr. P. Boshoff
Mr P. Gevera
Ms C. Koki
Mr. T.V. Makhubela
Mr. L. Mashamba
Mr A. Mgoqi
Ms. R. Shelembe
Mr. N.K. Singo
Mr S. Terblanche
Mr. M. de Villiers

Mr E. Adeneyi
Mr A. Bukanga
Mr. C. de Kock
Ms P. Kekana
Ms. J. Lum
Ms. N. Masangane
Mr A. Matiane
Mr. M. Mphaphuli
Ms G. Naude
Mr N. Nendouvhada
Ms. B. Ntlhoro
Ms. V. Nxumalo
Ms. A. Opperman
Ms. L. Ravhura
Mr. F. Kruger
Mr. C. Schalkwyk

Mr. M. Tsunke
Mr. E. Rammilla
Mr. T. Mabundza
Mr. A. Bukanga
Mr. N. Vafeas
Mr. C. Vongani
Ms S. Zardad

Dr. F. Ossa Ossa
Dr. B. Eickmann
Dr. A. Gucsik
Mr. J. Fitschen
Mrs G. Vieira da Costa

Dr. H. Wabo
Dr. F. Humbert
Ms L. Bowden
Mr. S. Fitzpatrick
Mr. T. Lechekoane
Ms F. Monareng

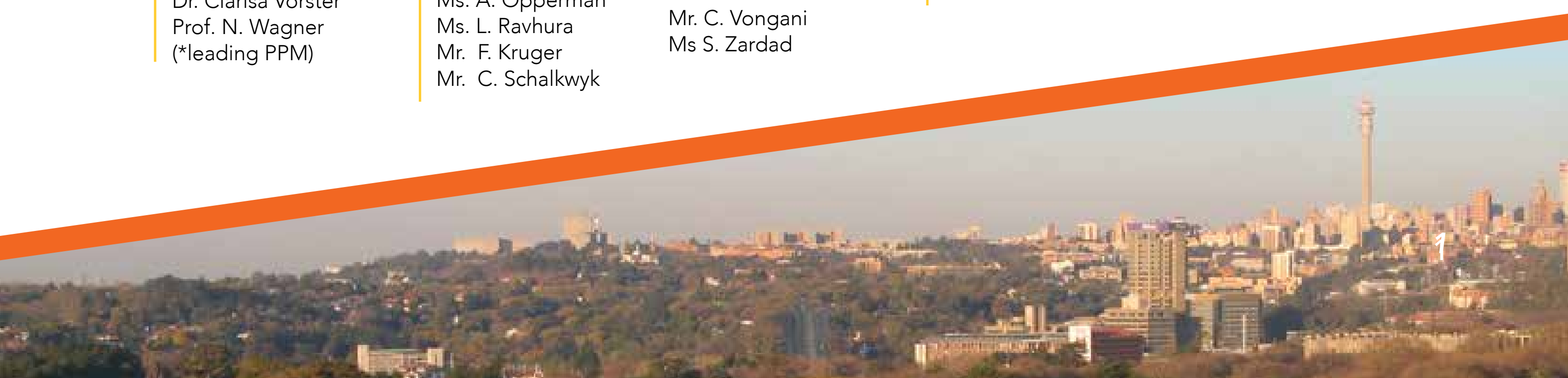

RESEARCH HIGHLIGHTS AND NEWS

Coal Petrography

In 2015, 6 Msc student registered to undertake coal related projects at UJ under the supervision of Prof Wagner. Most projects use coal petrography as the main analytical tool. Projects include: 1) Lateral comparison of coal composition in Botswana coalfields through the use of coal petrography (in collaboration with Analytika Holdings, Botswana, funded via CIMERA); 2) Petrographic consideration of the impact of the Tshipise fault on coal quality in the Soutpansberg coalfield (in collaboration with CoalofAfrica; funded by TESP Eskom grant); 3) A Chronological Study of the Effect of Oxidation on Coal in an Underground Mine (in collaboration with Sasol; funded by Sasol); 4) Petrographic study of Waterberg coals during heating (topic still to be refined) (in collaboration with Exxaro; funded by Exxaro); 5) Consideration of Rare Earth Elements (REE's) associated with coal and coal ash in South Africa. (funded by CIMERA); 6) The temporal and spatial variation of coal quality and mineability, with the focus on the Mpumalanga Coalfields (funded by CIMERA).

Other research projects for non-degree purposes include: 1) Production of a southern African coal and carbon petrographic atlas (printing funded by Coaltech, in collaboration with Wits and CGS); 2) Successful award of a ERA-MIN project with an international consortium for a project "Coal char as a substituting material of natural graphite in green energy technologies" (to commence in 2016). Small consulting projects requiring petrographic analyses were also undertaken, as well as detailed coal petrography for students registered at other academic institutions (Wits, UP) and with other supervisors. These projects included petrographic assessments of the Wankie coalfield and the Springbok Flats coalfield, assessment of the impact of a dolerite dyke on coal properties, and shale gas exploration projects.

In 2016, Prof Wagner received full ICCP accreditation for single coal analysis (SCAP), blend coal analysis (CBAP), and vitrinite reflectance of dispersed organic matter (DOMVR). She was also elected onto the ICCP Council as the new Editor of the ICCP Newsletter.

Installation of the multicollector inductively coupled mass spectrometer (MC-LA-ICP-MS)

The Nu Instruments Plasma II machine was delivered in the first week of October 2015. The very careful measurements of the C1 Lab goods lift taken by Marlina Elburg proved accurate, and the largest component, after uncrating, fitted with 2 cm to spare. Other challenges came up from time to time, such as a forklift being the only suitable way to position the magnet (see figure). The first ion beam was signaled just a week after start of the assembly, and there followed a long series of tests related to the set specifications, which were all met. Long (maintenance) and short (user) courses were subsequently run, with participants from Wits also taking part in the latter: cooperation with the Wits School of Geosciences is an essential part of this isotope project, as Wits is constructing an untraclean laboratory. While awaiting the arrival of the laser the instrument was immediately put to use for analyses from solutions. Inportantly, CIMERA agreed to fund the salary of an instrument scientist to take care of the laser and MC-ICP-MS combo, and late in 2015 the interviews took place and Ms Henriette Ueckermann, a South African who has gained extensive experience with this type of instrumentation in several countries in Europe, was offered and accepted this position which is crucial to the success of the project.

Prof. Marlina Elburg precisely positioning the 450 kg magnet as it is held aloft using a forklift

Medical Geology goes international

As medical geology is not available as a student research topic in many countries in Africa, the appeal of the subject has reached outside our borders and in 2015 two MSc students from Kenya, Ms Christa Koki and Mr Patrick Gevera, have joined Prof. Mouri's Medical Geology team, both researching topics related to rural communities in Kenya.

The Homo naledi discovery and PPM's involvement

In September 2015 the discovery and description of the Homo naledi fossils from the Rising Star cave system near Sterkfontein was given worldwide publicity, and of particular interest was the conclusion drawn by the team that this species, although small-brained, possessed a culture that apparently involved disposal of the dead.

Although Wits University hosted the media event, there was significant UJ involvement in the work. In the Faculty of Health Sciences, Dr Shahed Nalla carried out part of the descriptive and interpretive work on the fossils themselves. The PPM involvement goes back to the very beginning. Mr Pedro Boshoff, a team leader in the systematic cave exploration programme conducted by Prof Lee Berger, let down a camera on a string to where Rick Hunter and Stephen Tucker had entered the Dinaledi Chamber. He realized that a mandible pictured was possibly hominin, and alerted Prof. Berger. The connection is that Pedro Boshoff is also a part-time MSc student in PPM, studying speleogenesis. Later, Georgy Belyanin and Tebogo Makhubela carried out detailed mineralogical and geochemical studies on cave earth ('soil') in different parts of the cave system. They found that, while the floor in most parts of the system is dominated by fine quartz sand obviously derived externally, the froor of the Dinaledi Chamber, where the fossils were found, is very different: it consists mainly of fragments of mudstone derived internally (remnants of layered mudstone deposits still adhere to the walls of the chamber), and is effectively devoid of components derived from outside the cave. This became one of the important pieces of evidence, in the paper on the geological and taphonomic context, for the conclusion that the fossils could not have been transported into their present position by any natural process.

A NEW TEXTBOOK PUBLISHED

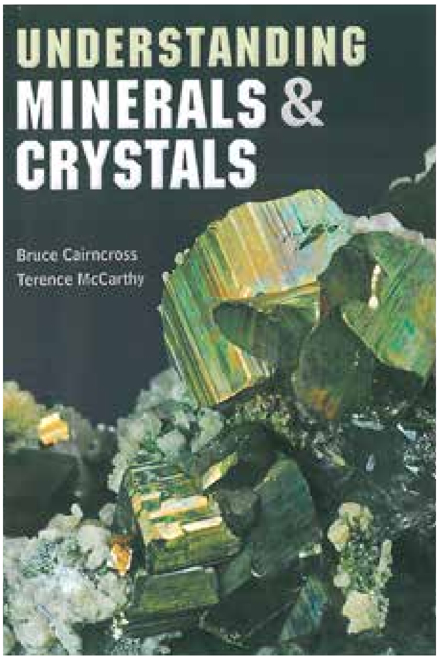

Cairncross, B. and McCarthy, T.S. (2015). **Understanding Minerals & crystals**. Struik Nature Random House Struik Natural History Publishing, Cape Town, 312 pages.

This book first provides an introduction to chemical bonds within crystals, the reason why crystals form and the conditions under which they form. It further discusses crystal and mineral properties, and includes a mineral identification key based on these. The second part deals with systematic descriptive mineralogy, detailing over 80 important minerals with excellent illustrative material. This is an undergraduate textbook as well as a vademecum for any mineral enthusiast.

RESEARCH PROJECTS AND PROGRESS

Geometallurgy and Economic Geology

A GEOMETALLURGICAL ASSESSMENT OF THE P1 AND P2 UNITS OF THE PLATREEF AT LONMIN'S AKANANI PROJECT, NORTHERN LIMB, BUSHVELD COMPLEX

G. Boikanyo Motloba, Fanus Viljoen and Bertus Smith

The Akanani prospect is situated in the Central Sector of the Platreef on the northern limb of the Bushveld Complex [1]. Mineralisation is primarily restricted to the P1 and P2 geological units of the Platreef at Akanani. Mineralisation in the P1 Unit is erratic, and occurs over a wide vertical interval. In contrast, the overlying P2 unit is more uniformly mineralised, with generally higher grades than P1.

Previously published studies of the Platreef focused mainly on an understanding of its geology and mineralogy, with published insights into its processing behaviour being comparatively rare. The present study therefore aims to investigate the geometallurgical nature of the P1 and P2 units of the Platreef at Akanani, with a focus on the influence of various ore properties (mineralogy, sulphide grain size, sulphide liberation) on the recovery of the platinum group elements (PGE), as well as nickel (Ni), copper (Cu) and sulphur (S).

Various ore types were sampled. These include feldspathic, serpentinised and olivine bearing pyroxenite occurring in P1 and P2 units. Orthopyroxene, clinopyroxene and plagioclase are the dominant primary silicate minerals, with serpentine the dominant secondary silicate. Base metal sulphides comprise dominant pyrrhotite, along with pentlandite and chalcopyrite. The size distribution of the sulphides is variable, with the finest encountered in the serpentinised pyroxenite, and the coarsest sulphides occurring in the feldspathic pyroxenite. Milling times, required to reduce these ore types to 60% passing 75 micron, are variable, with feldspathic pyroxenite milling the fastest, and serpentinised pyroxenite the slowest. Levels of liberation upon milling are comparatively poor for the serpentinised pyroxenite, and significantly better in the case of the feldspathic pyroxenite. This is mirrored by the recovery of the PGE from the various ore types, with poor recoveries associated with the serpentinised pyroxenite and better recoveries associated with the feldspathic pyroxenite.

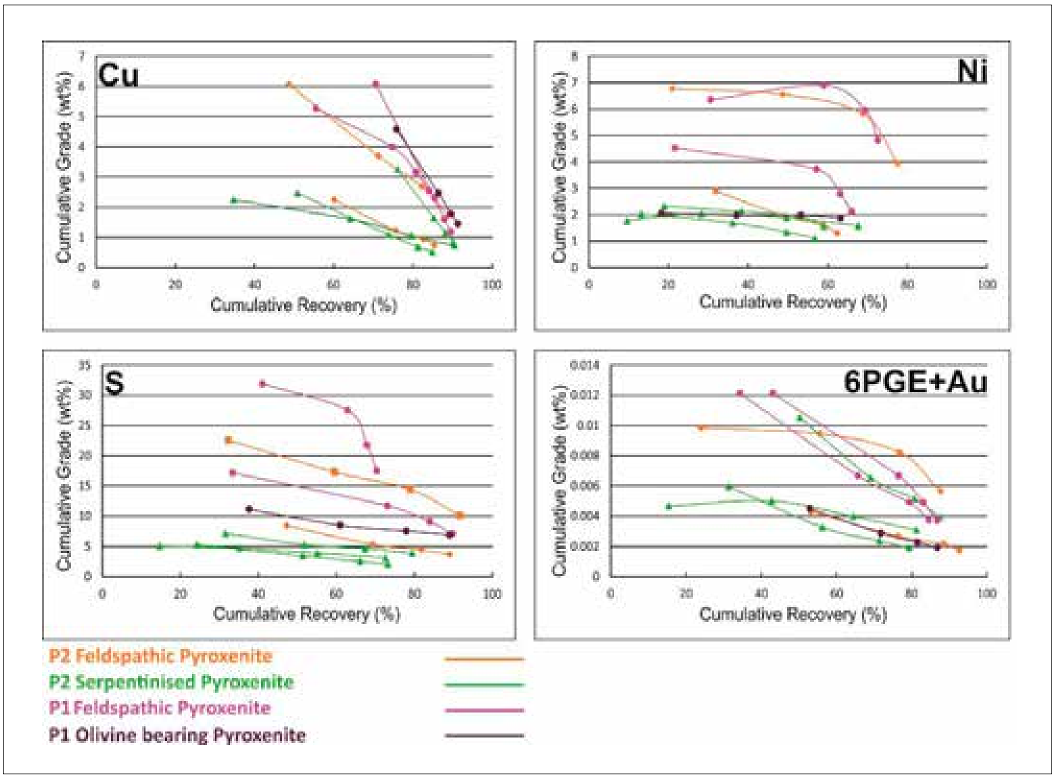

Figure 1: Cumulative concentrate grade as a function of cumulative recovery, for the samples collected from P1 and P2 at Akanani.

References:
[1] Yudovskaya et al. (2011) The Canadian Mineralogist 49:1349-1384.
[2] Xiao, Z. and Laplante, A.R. (2004) Minerals Engineering 17:961–979.

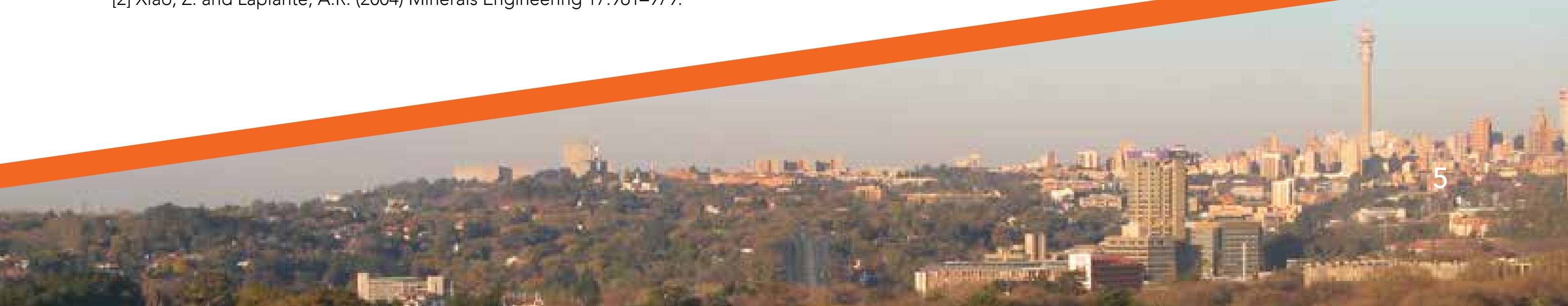

A GEOMETALLURGICAL STUDY OF THE MINERALIZED FOOTWALL UNDERLYING THE BRAKSPRUIT FACIES OF MERENSKY REEF AT THE LONMIN KAREE PT MINE, BUSHVELD COMPLEX, SOUTH AFRICA

M. Ernest Moitsi, Fanus Viljoen and Mike Knoper

The geological and mineralogical characteristics as well as the metallurgical (flotation) response of mineralised footwall [platinum group elements (PGE), gold (Au), sulphur (S), copper (Cu), nickel (Ni)] to Merensky Reef at the Karee Mine of Lonmin PLC, was investigated. Local grade of 2-4 g/t 6PGE is encountered in the mineralised footwall, which compares with a facies grade of ~7 g/t 6PGE in the overlying Merensky Reef. The continuity of this style of mineralisation is poorly understood, resulting in increased uncertainty of grades and recovery prediction in considering processing of this ore type, leading to a lack of predictive capability when dealing with this ore type in processing.

Various geological and metallurgical parameters such as mineralogy, grain size distribution, liberation upon milling, and flotation response, were determined, and compared to the overlying Merensky Reef (the Brakspruit facies type). Base metal sulphides in the footwall (the likely host of the platinum group elements) comprise of dominant pyrrhotite, along with pentlandite and chalcopyrite. These are finer grained in the footwall than in the Merensky Reef. Footwall ore material mills faster than ore from the Merensky Reef (in order to achieve a target grind of 60% passing 75 micron, commonly used throughout the Bushveld Complex for the processing of Merensky Reef ores [1]). Liberation of sulphides upon milling is lower for the footwall than for the Merensky Reef. The flotation efficiency is also lower in the footwall than for Merensky Reef (i.e. lower concentrate grades are encountered in the initial stages of flotation) (Figure 1), which is likely a consequence of the lower level of liberation of the footwall upon milling, relative to Merensky Reef.

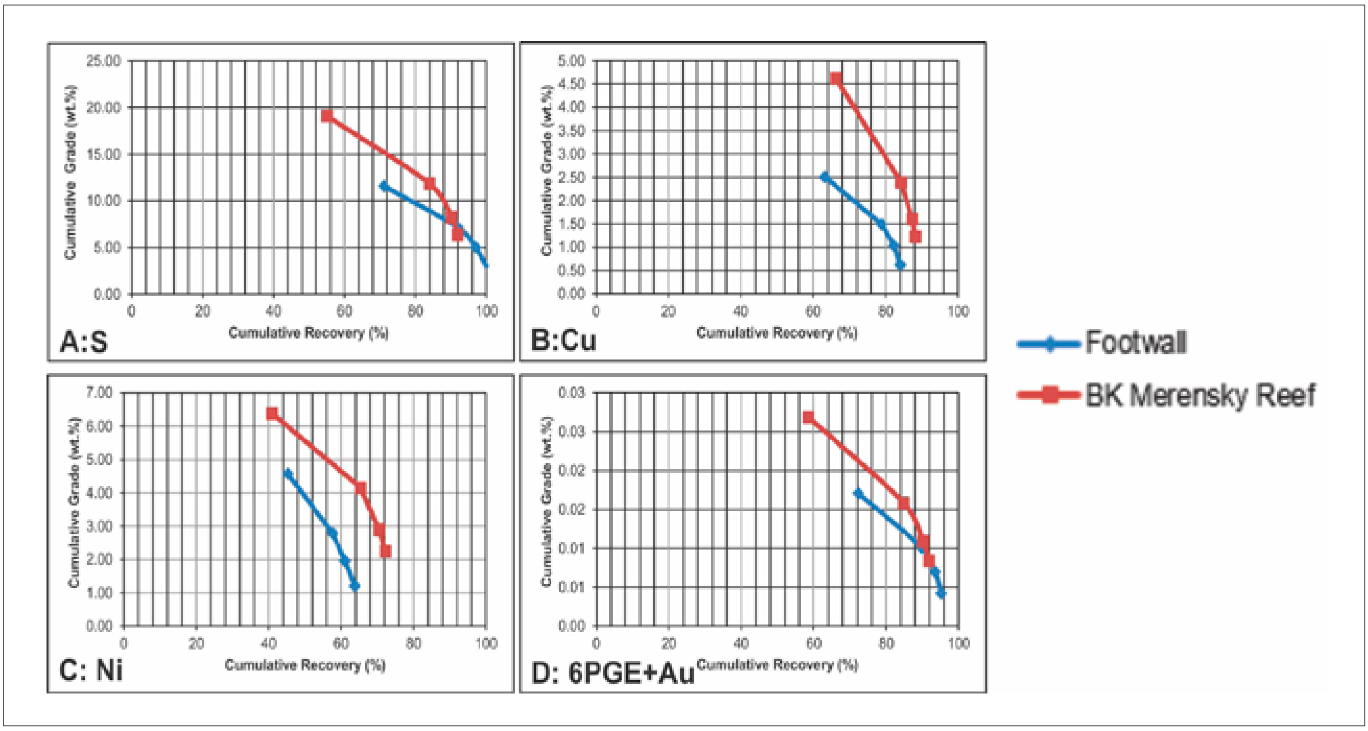

Figure 1: Cumulative concentrate grades (wt.%) as a function of cumulative recovery (%) for bench top flotation tests conducted on mineralised footwall and Merensky Reef.

References

[1] Wiese et al. (2005) Minerals Engineering 18: 189-198.

UNUSUAL MANGANESE ENRICHMENT IN THE MESOARCHEAN MOZAAN GROUP, PONGOLA SUPERGROUP, SOUTH AFRICA

Frantz Ossa Ossa[a,1], Axel Hofmann[a], Olivier Vidal[b], Jan D. Kramers[a], Georgy Belyanin[a], Barbara Cavalazzi[a,c].

[a]Department of Geology, University of Johannesburg, Auckland Park 2006, Johannesburg, South Africa;
[b]LGCA, UMR 5025, Université Joseph Fourier, 1381 rue de la Piscine, BP 53, F-38041 Grenoble Cedex 09, France;
[c]Dipartimento di Scienze Biologiche, Geologiche e Ambientali, Università di Bologna Via Zamboni 67, 40126 Bologna, ITALY;

An unusual manganese deposit is described, associated with unweathered rocks of the Mesoarchean Mozaan Group (Fig. 1), Pongola Supergroup, South Africa. The observed MnO contents can reach 15 wt.%. These values are interpreted as resulting from the hydrothermal alteration of ferruginous shale and BIF parent rocks, the primary MnO contents of which were as high as 8.53 wt.%.

A detailed mineralogical and petrographic study shows that these parent rocks are characterized by manganoan siderite and other Mn-Fe-rich mineral phases such as kutnahorite, Fe-Mn-chlorite, magnetite and pyrite (e.g. Fig. 2). In the absence of supergene processes, their thermal alteration allows a diversification of mineral assemblages where ferroan tephroite, calcian rhodochrosite, rhodochrosite, pyrochroite, jacobsite, manganite, pyrophanite, cronstedtite, manganoan Fe-rich chlorite, manganoan phlogopite, hematite and pyrite may replace partially or totally the previous mineral assemblage (e.g. Fig. 2).

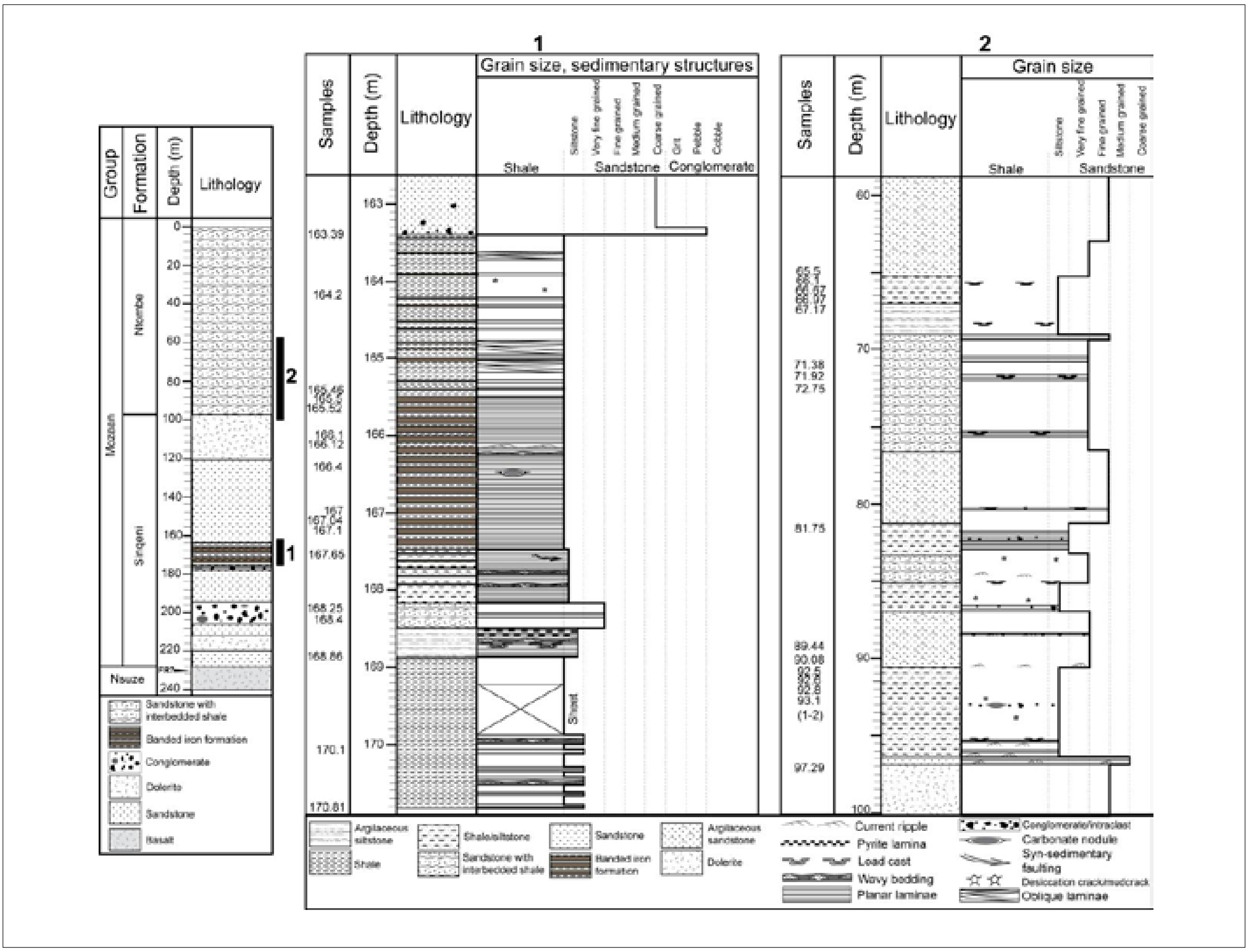

Fig. 1. Stratigraphic column of drill core TSB07-26 of the lower Mozaan Group and details of the studied successions of the Sinqeni Formation (1) and Ntombe Formation (2).

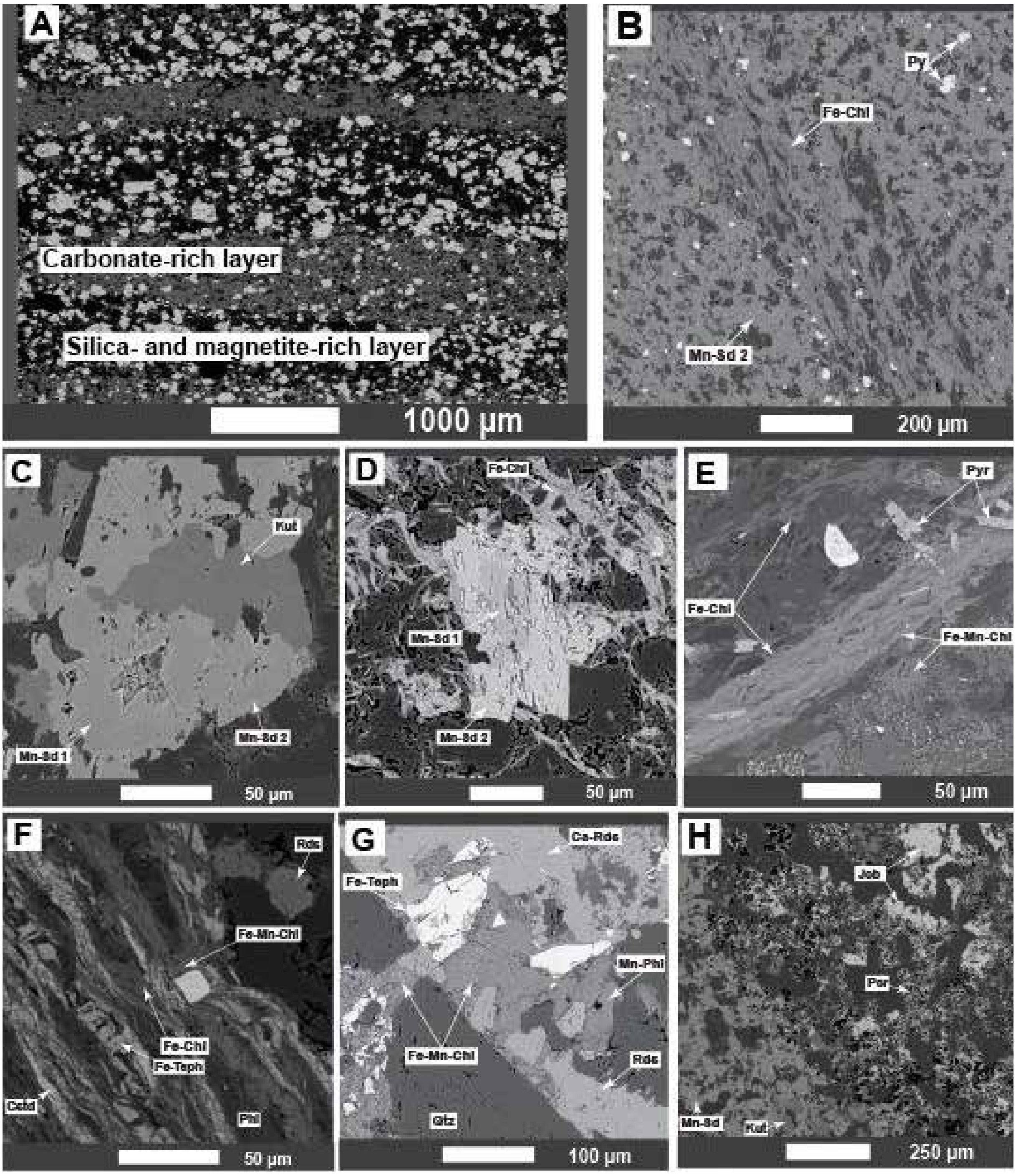

Fig.2. Characterization and relationship between mineral phases in the Mozaan Group. **A**. Backscattered electron image of carbonate-rich lamina interlayered with silica- and iron oxide-rich lamina. **B**. Backscattered electron image of carbonate-rich shale bed characterized by manganoan siderite (Mn-Sd 2), pyrite (Py) and Fe-rich chlorite (Fe-Chl) in foliation domains. **C-D**. Backscattered electron image showing manganoan siderite (Mn-Sd 1&2) associated with kutnahorite (Kut) in image C. **E-F**. Backscattered electron images of late metamorphic phases, including Fe-Mn-Chlorite (Fe-Mn-Chl), pyrophanite (Pyr), cronstedtite (Cstd) and rhodochrosite (Rds) partially replacing early metamorphic phases that include Fe-chlorite (Fe-Chl) and phlogopite (Phl) defining the foliation. G. Backscattered electron image of fracture fillings characterized by ferroan tephroite (Fe-Teph); rhodochrosite (Rds); cronstedtite (Cstd); manganoan phlogopite (Mn-Phl) and quartz (Qtz). H. Backscattered electron image showing early carbonate phases, Mn-Sd 2 and kutnahorite (Kut), partially or totally replaced by late pyrochroite (Pcr) and jacobsite (Jcb).

Thermodynamic modeling performed on chlorite phases associated with the described mineral assemblages illustrates a decrease of average crystallization temperatures from ca. 310 ± 54 °C at early metamorphic stages to ca. 244 ± 41 °C in mineral phases associated with late fluid circulation (Fig. 3). This suggests that an event of retrograde metamorphism involving fluid circulation or hydrothermal alteration post-dating metamorphism could have controlled mineral transformation processes. Such a mineral transformation would have been accompanied by local metal remobilization allowing a progressive Mn enrichment from unaltered parent to altered rocks (Fig. 3).

Type of paragenesis	Major minerals		Minor minerals		Temperature of formation (°C)	Thermal stage	Inferred age
	Phases	MnO (wt.%)	Phases	MnO (wt.%)			
Paragenesis 1	Fe-rds	30				Diagenesis	Mesoarchean
Paragenesis 2	Mn-sd Fe-chl	9 < 1	Kut Ank	18 5	310 ± 54	Metamorphism 1	Late Archean *(Elworthy et al., 2000; Hofmann et al. 2015)*
Paragenesis 3	Mn-Fe-chl Mn-sd Fe-teph Rds	2 17 30 51	Pyr Cstd	22 6	264 ± 34	Metamorphism 2	Mesoproterozoic *(present study)*
Paragenesis 4	Mn-Fe-chl Mn-sd Fe-teph Ca-rds Pcr Jcb	7 19 34 38 77 13	Ank Pyr Cstd Mn-phl	5 33 6 5	244 ± 41	Late fluid circulation	

Fig.3. Synthesis of Mn-rich mineral parageneses and thermal events related to their occurrence

$^{40}Ar/^{39}Ar$ dating suggests that a late, separate hydrothermal event could have controlled mineral transformation and related Mn enrichment between about 1100 and 1500 Ma ago (Figs. 3 and 4). Ferruginous shale and BIFs of the Mozaan Group may represent an exceptional example for Archean manganese deposits belonging to the oldest known examples of Mn deposition. This study shows for the first time that, in the absence of supergene processes, low grade manganese associated with Mesoarchean sedimentary formations of the Kaapvaal Craton could represent a primary constituent related to the deposition in a shallow marine environment where oxygenic photosynthesis would have acted as a first-order control during Mn precipitation. Such a hypothesis opens a new window for a better constraining of the redox conditions in seawater, as well as oxygen levels in the atmosphere-hydrosphere system during the Archean Eon.

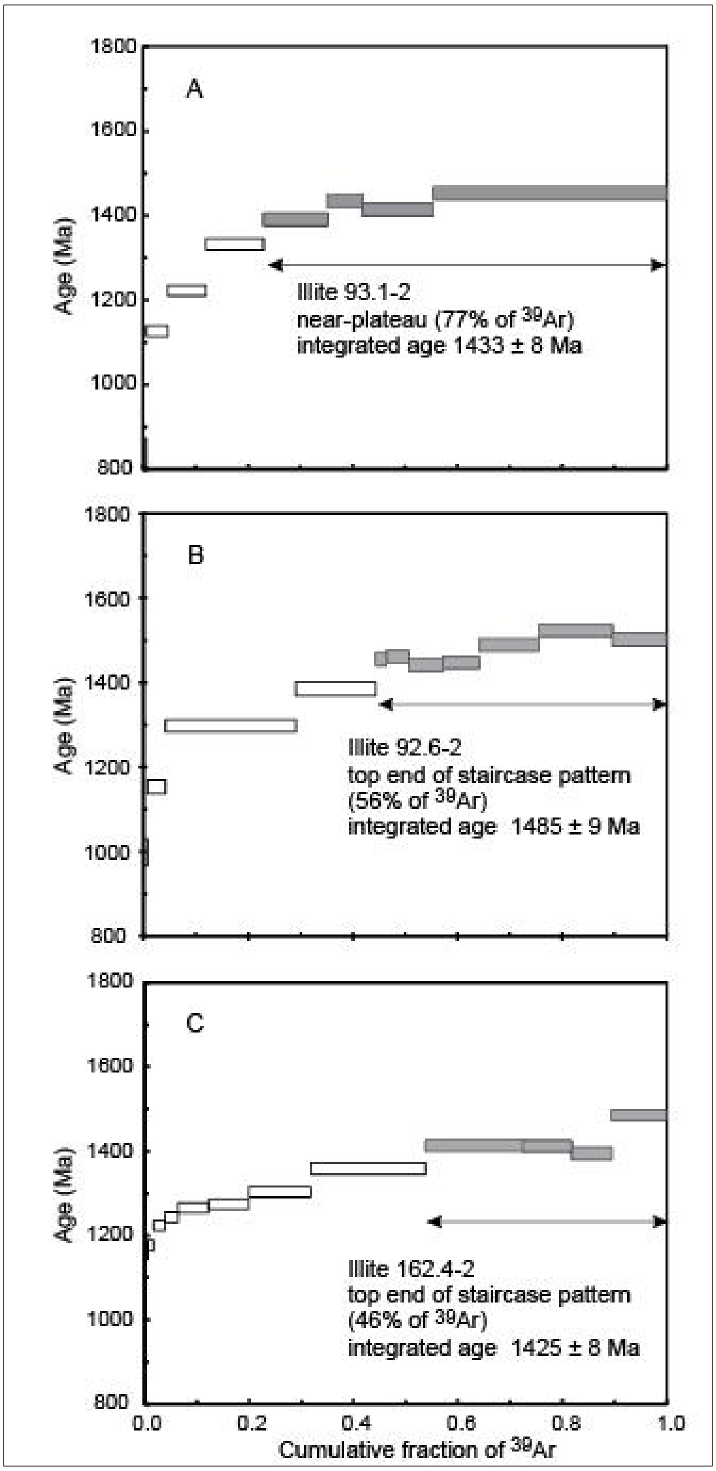

Fig. 4. Stepwise heating age spectra of aliquots of the <2 μm illite fraction from samples 162.4, 93.1 and 92.6 (see Fig. 1). Error boxes reflect 95% confidence limits. Note general staircase nature of the patterns and broad consistency of the ages reflected by high temperature steps.

A PETROGRAPHIC AND GEOCHEMICAL ANALYSIS OF THE KALAHARI MANGANESE DEPOSIT, NORTHERN CAPE, SOUTH AFRICA

Lauren C. Blignaut, Fanus Viljoen and Harry Tsikos

The largest and most significant deposit of the ± 2220 Ma Kalahari Manganese Field (KMF) is the 320 km_2 Kalahari Manganese Deposit (KMD). The manganese (Mn) is exploited from three beds that are interbedded with hematite lutite and banded iron formation [1]. The northern KMD ores were affected by hydrothermal alteration, involving carbonate dissolution and the removal of CO_2, and the introduction of alkali elements, base metals and iron into the system [2]. Normal and thrust faults were important in localising the alteration system, as they acted as conduits for hydrothermal fluids [3]. However, these were not the only factors that contributed to the alteration of the ores. Another possibility for this enrichment involved the flow of isotopically light fluid throughout large parts of the KMF, which was related to the Hotazel/Olifantshoek unconformity [4]. The Mn is divided among the low-grade Mamatwan and the high-grade Wessels-type ores, with the latter being constrained to the northern part of the KMD [5]. The lowermost Mn bed is the thickest and most Mn-rich and, thus, most favourable for mining [1]. A thorough understanding of the ore (the genesis and alteration of the ore, which includes both the upper and lower ore bodies, the spatial distribution of the mineral assemblage, as well as the fluid-rock interactions) is essential, in order to optimize exploitation and maintain the high quality and quantity output of the ore.

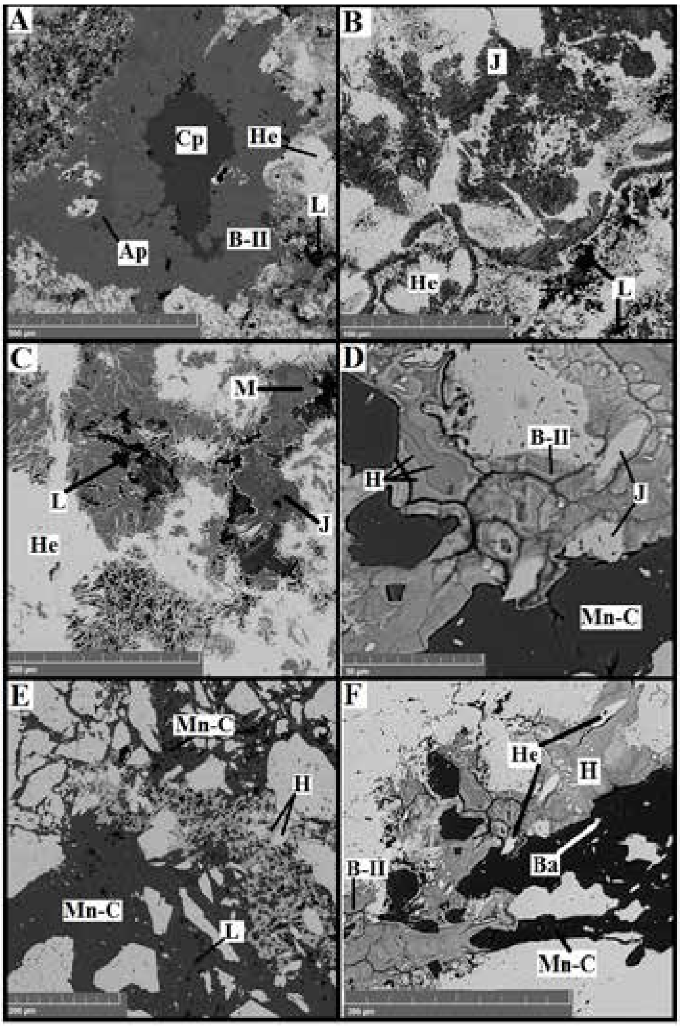

Figure 1: Mineralogical and textural associations of the upper bed. BSE images of N94I_14 (A) coarse-grained hematite matrix with inclusions of lizardite. Braunite-II with caryopilite (Cp) core with inclusions of apatite. (B) Subhedral hematite patches enclosed in 'needle-like' jacobsite with interstitial lizardite. (C) Fine-grained, needle-like hematite intruding into the jacobsite and manganite grains with lizardite inclusions. BSE images of the lower bed of (D) N94I_21; Mn-calcite and jacobsite patches enclosed by 'oolitic-type' textures or layers of variable hausmannite. (E) N94I_21; Mn-calcite veining with lizardite inclusions and an intergrowth of the hausmannite matrix. (F) N94I_21; Mn-calcite veining with interlayering of differing hausmannite fluid structures or layers, with inclusions of hematite and barite.

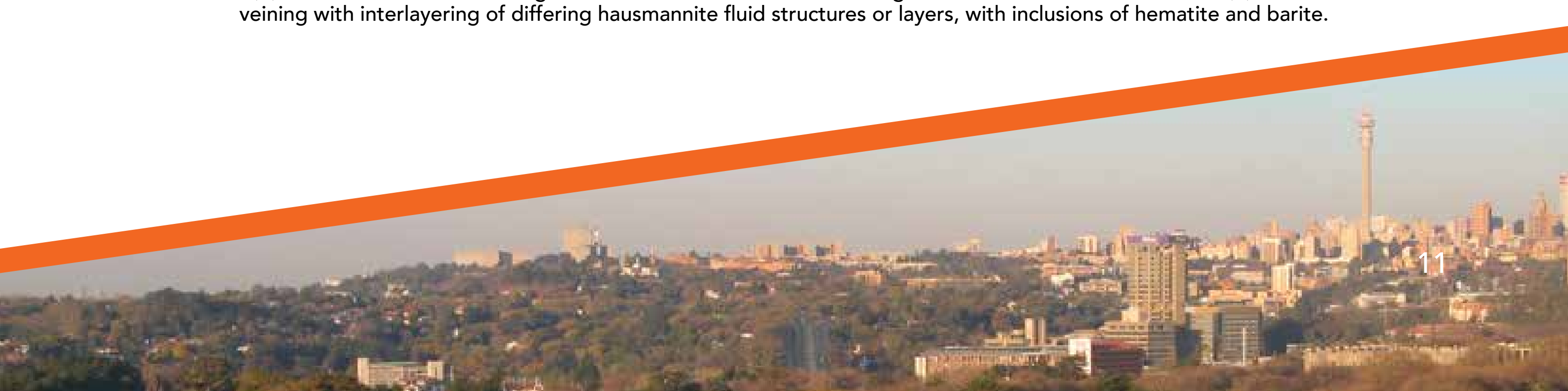

Oxides, carbonates, hydroxides and silicates dominate the mineralogy of the Mn beds (Fig. 1). The protolith and low-grade ores are comprised of a braunite-kutnohorite-hematite assemblage, with coarse-grained carbonate ovoids, lenticles and laminae. The high-grade ores, however, are composed of a braunite-II-bixbyite-hausmannite assemblage with minor hausmannite and calcite textural features. Mn_3O_4, Fe_2O_3, CaO, MgO and Fe_2O_3 dominate, with an overall increase in Mn_3O_4 and Fe_2O_3, and a decrease in SiO_2, MgO and CaO with increasing ore grade. The depletion of these elements indicates carbonate leaching, as well as the replacement of braunite by braunite-II, bixbyite and hausmannite during the Wessels alteration event [1]. The upper body contains higher Fe_2O_3 and SiO_2 abundances, suggesting a possible BIF-dominated environment, whereas higher CaO abundances in the lower body indicate a possible carbonate depositional environment. The trace elements vary significantly with ore grade and depth. Only Ba, Sr and B show an evident increase in concentration from the protolith to the high-grade ore, suggesting an addition of these elements by fluid. Boron (B) in particular is an important component of this study, as concentrations >400 ppm are highly detrimental to the steel quality. B abundances fluctuate between the Mn beds, but overall shows a higher average abundance within the upper bed. B maybe mineralogically controlled as the highest concentrations show large abundances of braunite/braunite-II, gaudefroyite and bixbyite. Rare Earth Element (REE) analysis indicates enrichment in heavy over light REE, and an overall increase in REE with an increase in alteration. The REE signature is similar to that of the present day deep ocean level seawater.

References:

[1] Beukes N.J (1983) Development in Precambrian Geology, 6, 131-209.

[2] Evans D.A.D et al (2001) Economic Geology, 96, 621-631.

[3] Kleyenstüber A.S.E (1993) Resource Geology, 17, 2-11.

[4] Tsikos, H (2003) Economic Geology, 98, 1449-1462.

[5] Kleyenstüber A.S.E (1984) Transvaal Geological Society of Southern Africa, 87, 257-27

CLASSIFICATION OF DIAMOND SOURCE ROCKS IN THE WAJRAKARUR KIMBERLITE FIELD OF SOUTHERN INDIA, USING MINERAL CHEMISTRY

Dongre, A.N. and Viljoen, K.S.

The mostly diamondiferous Wajrakarur Kimberlite Field (WKF) of Southern India comprises about 30 kimberlites. These represent widespread potassic intracratonic magmatism, emplaced mostly as pipes in Archean granites and gneisses. The nomenclature of these rocks remains controversial and they have been variously assigned as kimberlites (Group I), orangeites, lamproites and ultramafic lamprophyres. For the present study, twenty reasonably fresh kimberlites from the WKF field were examined in detail, and then classified using a mineralogical-genetic classification based on the IUGS classification scheme for igneous rocks [1,2]. All the pipes exhibit an inequigranular rock texture, with macrocrystic and megacrystic olivines occurring in a finer grained matrix of phenocrystic olivine, as well as variable quantities of groundmass spinel, perovskite, monticellite, carbonate, phlogopite, clinopyroxene and Ti- rich garnets. The presence of abundant olivine (macrocrysts and phenocrysts), primary calcite, perovskite, monticellite, along with the Al- and Ti-poor nature of phlogopites and diopsides, as well as the absence of sanidine and K-richterite, precludes their classification as lamproite.

The presence or absence of groundmass clinopyroxene in these rocks (for example) have been used to discriminate Group I kimberlites from orangeites, lamproites and ultramafic lamprophyres. In the present study the distinction is based on mineral compositions. Groundmass clinopyroxene is abundant in 11 of the pipes, while it is absent in the remainder. The 9 pipes which do not contain clinopyroxene have low phlogopite abundances, along with strong Al_2O_3 enrichment (up to 20 wt. %) in the phlogopite, typical of Group I kimberlites. Spinels are mostly aluminous with Cr/(Cr+Al)<50 (molar) and falls into the magnesian ulvospinel trend (kimberlite trend 1) on the projected front face of the reduced spinel prism, again confirming a classification as Group I kimberlites. In contrast, one pipe in the Lattavaram cluster shows an Al and Ti enrichment trend in phlogopite and diopside which is typical of ultramafic lamprophyres (UML). In this instance the spinels are restricted to the 'titanomagnetite' trend (kimberlite trend 2) and are compositionally similar to those in the Sarfartoq UML's of West Greenland. The presence of amphiboles, diopside and Ti-Zr rich garnets in the rock groundmass also supports a classification as UML.

Clinopyroxene in the remaining 11 pipes are phenocrystic Al-Ti poor diopsides. These intrusions are also characterised by comparatively Al-poor phlogopite (up to 3 Wt. % Al_2O_3) which is typical for orangeites. Spinels are mostly chromian spinels with compositions Cr/(Cr+Al)>50, and fall into 'kimberlite trend 2' compositions, again typical of orangeites. Hence it is concluded that these intrusions are all closely related to orangeites ('Group II kimberlites'). This argument is supported by the presence of the Cretaceous TK1 pipe in the Timmasamudram cluster, which has an orangeite affinity [3]. Based on radiogenic isotope systematics, it is clear from this kimberlite that metasomatized subcontinental lithospheric mantle (the source of orangeite magmatism), was already in in existence at ~1100 Ma in the mantle below the WKF.

References:

[1] Le Maitre R (2002) *Igneous Rocks: a Classification and Glossary of Terms*. Cambridge University Press, 236.

[2] Tappe S et al. (2005) J Petrol 46:1893–1900

[3] Chalapathi Rao NV et al. (2015) Gondwana Res. *http://dx.doi.org/10.1016/j.gr.2015.06.006*

MODE OF URANIUM OCCURRENCE AND DISTRIBUTION IN COALS OF THE SPRINGBOK FLATS BASIN

Valerie Nxumalo[1,2], Jan Kramers[2], Clarisa Vorster[2], Bruce Cairncross[2] and Wojciech Przybylowicz[3,4]

[1] Council for Geoscience, Pretoria, South Africa

[2] University of Johannesburg, South Africa

[3] iThemba LABS, National Research Foundation, P.O. Box 722, Somerset West 7129, South Africa

[4] AGH University of Science and Technology, Faculty of Physics & Applied Computer Science, al. A. Mickiewicza 30, 30-059 Kraków, Poland

In a project focusing on the nature of the remarkably high uranium content in coals from the Vryheid Formation in the Springbok Flats basin, as well as the provenance of the associated clastic sediments, five boreholes were drilled that intersected all coal zones. While vein-type uranium mineralization was found in mudrocks overlying the uppermost coal zone (see PPM report for 2014), the nature of the demonstrable uranium mineralization in the coal itself (Figure 1) remained a mystery.

Figure 1 . Radioactive coal with calcite cleats and lenses of mudstones. Sample 3.2 from Borehole 3 with 1968 ppm U

We have carried out Proton Induced X-ray Emission (PIXE) analysis of coal using the proton microprobe at iThemba LABS in Somerset West to address this problem. The results (shown in Fig. 2 for one sample) demonstrate that U is not present in fractures or cleats, but is uniformly distributed in the coal matrix itself and thus it is highly likely that its enrichment is syngenetic. This has important consequences for any potential projects envisaging combined coal-uranium mining, or undeground coal gasification.

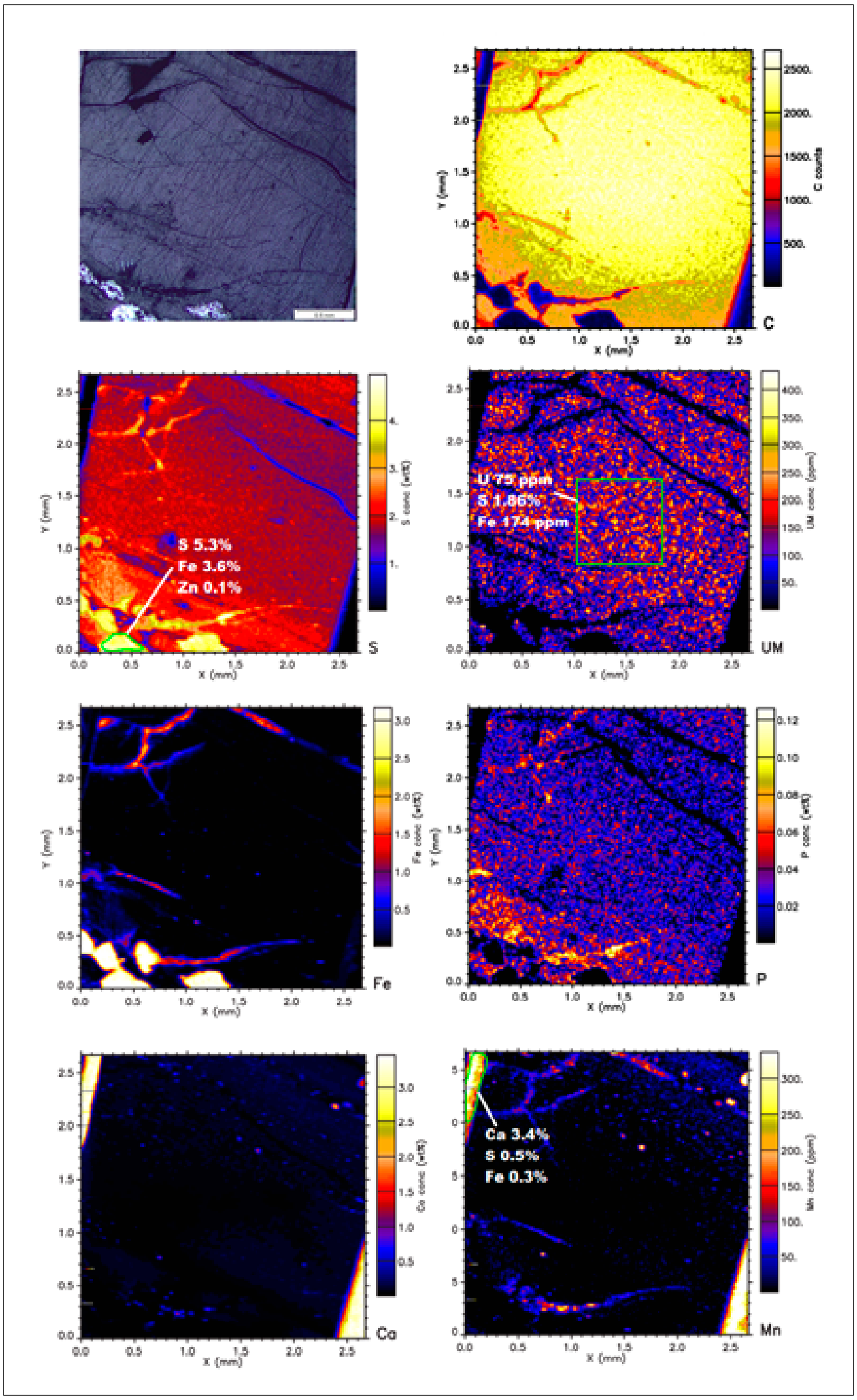

Figure 2 . Reflected light microphotograph and PIXE maps (C, S, U, Fe, P, Ca and Mn) of a coal sample as shown in Fig. 1. Uranium is seen to be disseminated in organic components in coal and not hosted in a discernible (> 1 μm) mineral phase, or in cleats.

The effect of dolerite intrusions on the shale gas potential of the Ecca Group in borehole from the central Karoo Basin.

Elijah Adeniyi, Nic Beukes and Michiel de Kock

The shale gas reserve of the Ecca Group has been estimated to be between 13Tcf to 485Tcf covering an area of about 155, 000 km^2. However, these estimates do not take into account the thermal effect of voluminous Jurassic-aged igneous intrusions within the basin. This research aims to quantify the changes in mineralogy and chemistry of Ecca Group mudrocks in proximity to dolerite intrusions in borehole PP47; about 1400meters deep, near Phillipolis in the central part of the Karoo Basin (S 30.29° E 025.24°). We report on a suite of analyses that include optical microscopy, x-ray diffraction (XRD) on bulk and oriented clay mineral separates, RockEval pyrolysis, Vitrinite Reflectance, total organic carbon content (TOC) and organic carbon isotopes ($\delta^{13}C_{org}$). The mudstones are poorly sorted and grain sizes range from clay to silt-sized particles. The dolerites are medium-grained, with euhedral rectangular laths of plagioclase, clinoproxene, poikilitic orthopyroxene, quartz, and pyrite. Pyrite is a prominent constituent in the mudstones close to intrusions. XRD analyses of mudrock samples reveal quartz, chlorite, illite, and feldspar as dominant mineral phases (Figure 1). Illite crystallinity measure with Kubler Index increases with depth and in proximity to dolerite accompanied by a decrease in chlorite abundance (Figure 2). TOC and $\delta^{13}C_{org}$ composition appear to be mainly controlled by lithological variation; the shales are enriched in TOC and $\delta^{13}C_{org}$ relative to siltstone. There is also an enrichment of $\delta^{13}C_{org}$ close to dolerite sills. RockEval and Vitrinite Reflectance (Figure 3) analyses indicate the presence of type III gas prone kerogen. The initial results show that the hydrocarbon transformation in this borehole is related to both the thermal evolution of the basin and the impact of the dolerite intrusions. Samples from the thermal aureoles of intrusions and from near multiple closely spaced intrusions have been most affected.

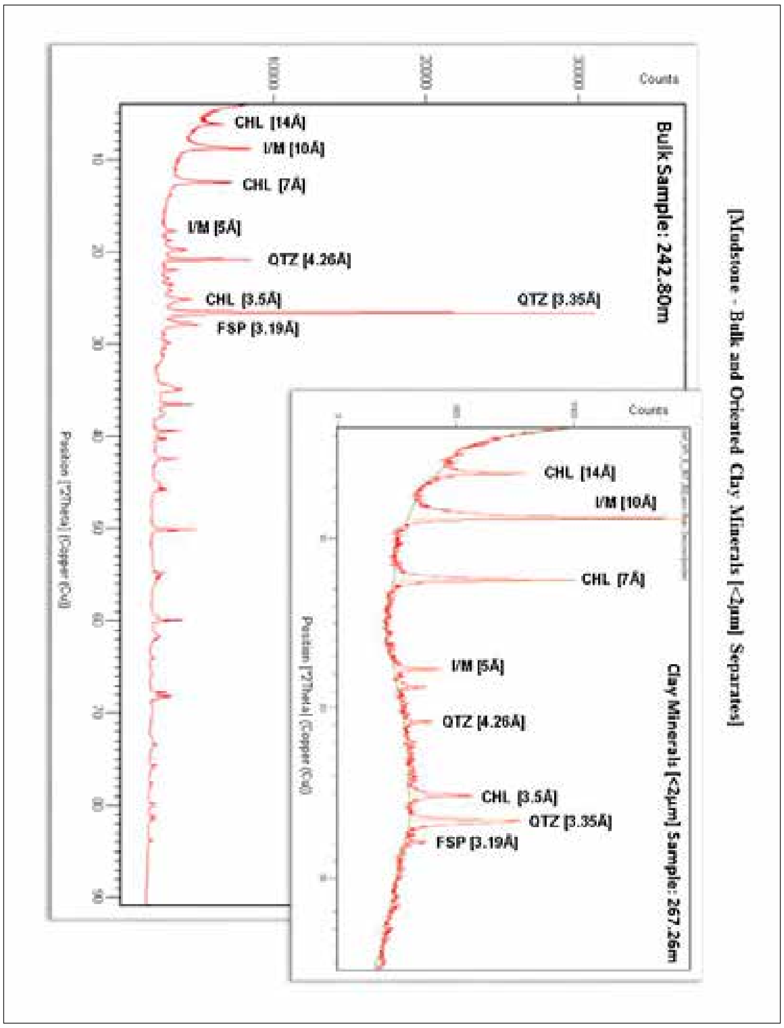

Figure 1: XRD diffractograms of the Mudstones Bulk and Oriented Clay Minerals [<2µm]. HL: Chlorite. I/M: Illite/Mica. OTZ: Quartz. FSP: Feldspar

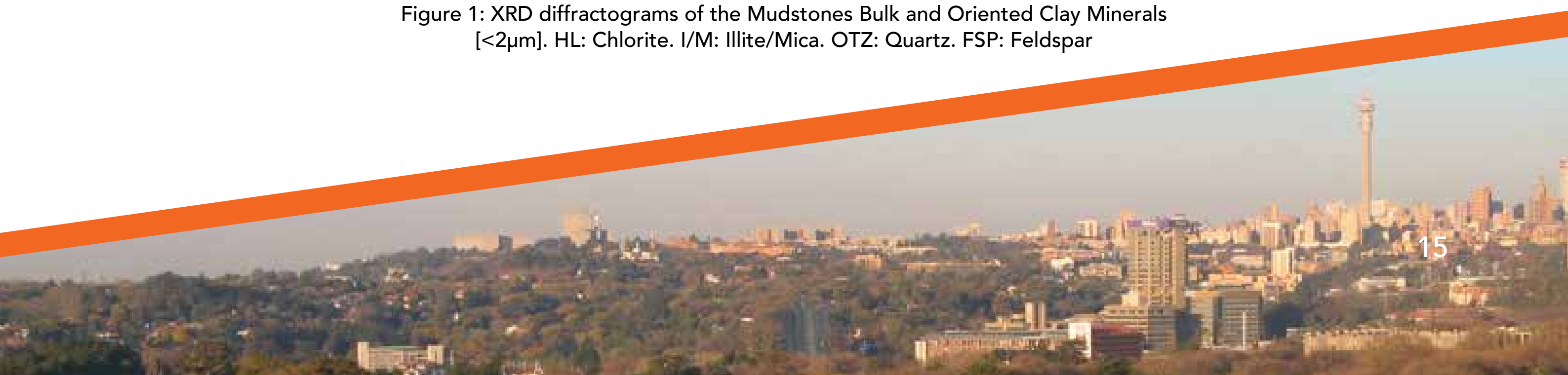

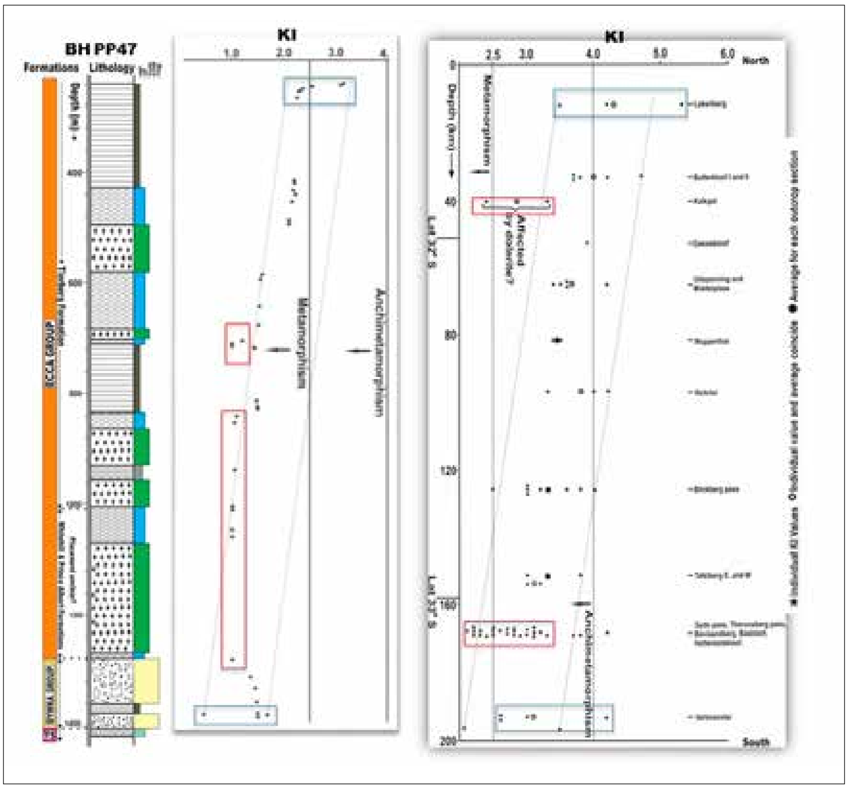

Figure 2: BH PP47 Kubler Index (Illite Crystalinity) plotted against Depth and compared with Western Bokkeveld Outcrops. (After A.V. Csaky) by Rowsell & de Swardt (1976) The KI index trends from the anchimetamorphism to metamorphism boundaries by depth **1. Global trend: 3** to **1.5** index values at the upper vs lower part of the borehole respectively. **2. Local trend:** KI **reduces** and **increases** around dolerite within the mudstone facies; particularly at the three lower sills

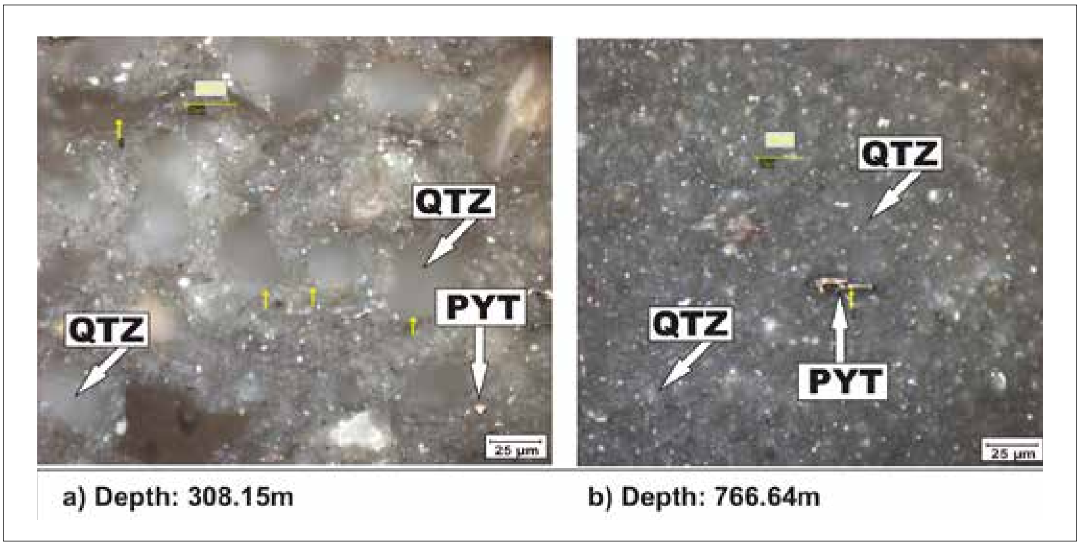

Figure 3. Samples 308.15m and 766.64m [far from intrusion]: No structure/orientation, very fine grained and scattered organic matter, coarser quartz particles and frambiodal pyrite in optical observations.

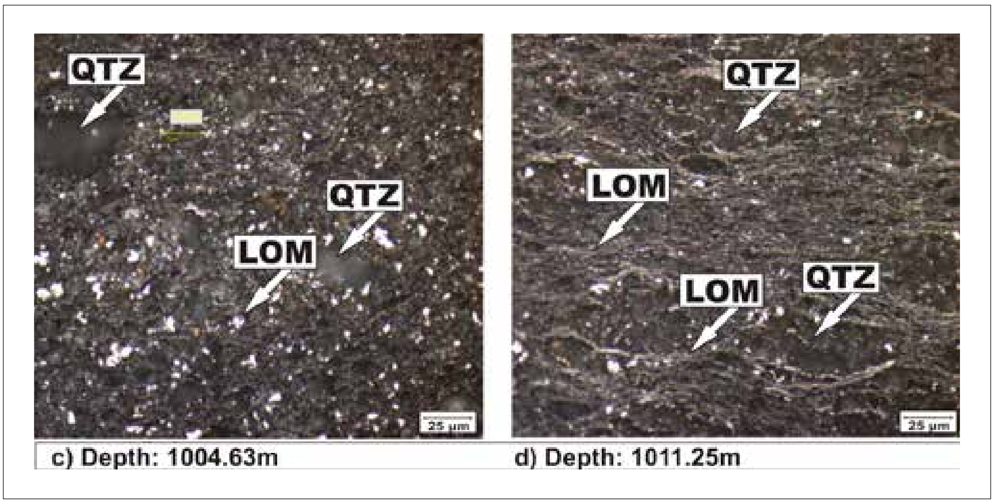

Figure 4. Samples 1004.63m and 1011.25m [close to intrusion]: Apparent orientation in organic matter structure, layered and networked around quartz particles with pyrite inclusions. They possess significant highly matured organic matter that appears as a solid bitumen network and with values that are consistent with gas generation zones.

MULTIFACTOR REVIEW OF NATURAL CARBONATE RESOURCES OF MALAWI FOR SMALL-SCALE PROCESSING

F. E. D. Senzani and A. F. Mulaba-Bafubiandi

A survey is being undertaken of all calcite-bearing carbonate occurrences in Malawi with a view to assess their potential for small-scale mining. Since the country is largely underlain by igneous and metamorphic rocks and clastic, non-carbonate sediments, the occurrences are few but a number are likely to be economically viable. Fig. 1 and 2 show all occurrences and the major ones, respectively.

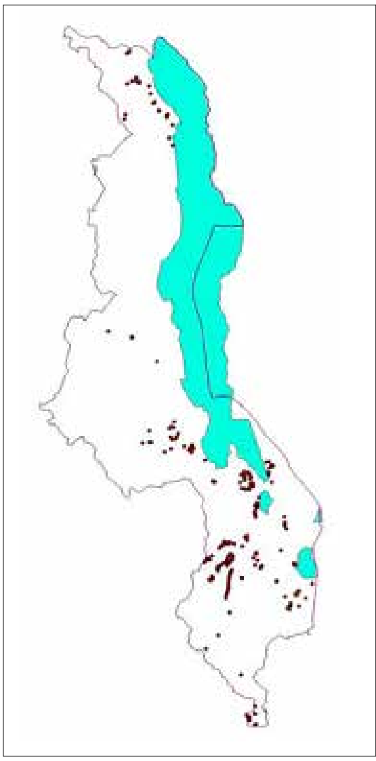

Figure 1. Localities of all calcite-bearing carbonate occurrences in Malawi.

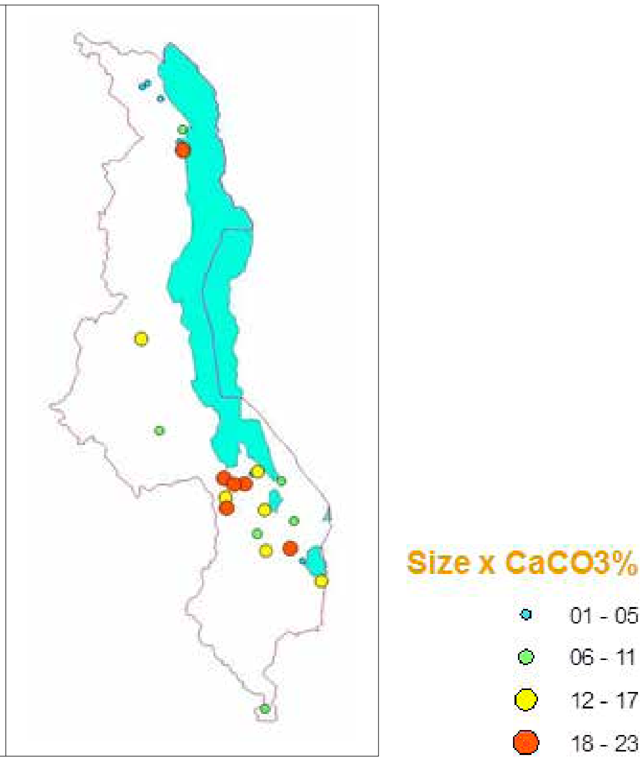

Figure 2. Main occurrences ranked according to surface outcrop size x $CaCO_3$ content.

Further factors to be considered in projecting economic viability of the deposits are distance from main roads, from the lake and/or from perennial rivers.

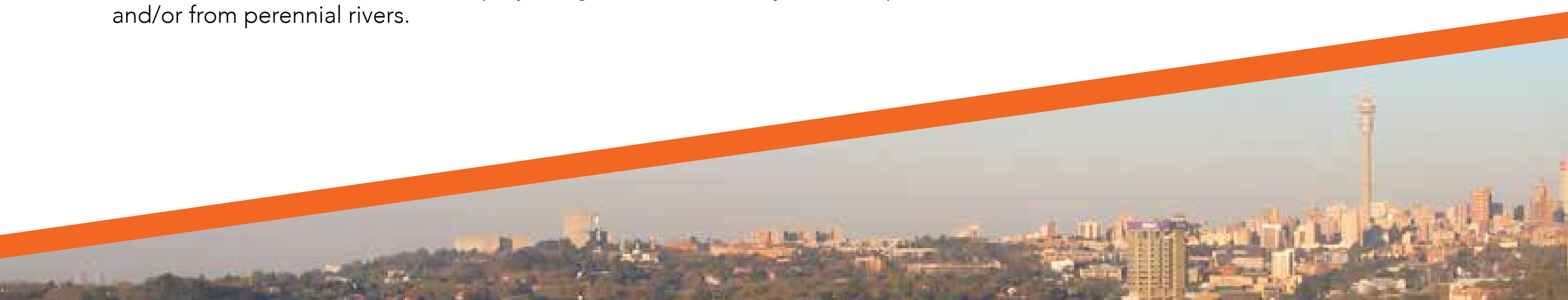

Magmatism, Metamorphism and Tectonics (and its Chronology)

DETACHMENT FOLDING OF PARTIALLY MOLTEN CRUST IN ACCRETIONARY OROGENS: NEW MAGMA ENHANCED VERTICAL MASS AND HEAT TRANSFER MECHANISM

Jérémie Lehmann[1,2], Karel Schulmann[3,4], Ondrej Lexa[3], Pavla Štípská[3,4], Pavlína Hasalová[3,5], George Belyanin[2], and Michel Corsini[6]

[1] EGRI, School of Geosciences, University of the Witwatersrand, PVT Bag 3, Wits, 2050, South Africa

[2] Department of Geology, University of Johannesburg, Auckland Park 2006, South Africa

[3] Centre for Lithospheric Research, Czech Geological Survey, Klárov 3, Prague 1, 11821, Czech Republic

[4] Ecole et Observatoire des Sciences de la Terre, Institut de Physique du Globe de Strasbourg – CNRS UMR7516, Université de Strasbourg, 1 rue Blessig, F-67084, Strasbourg Cedex, France

[5] Institute of Geophysics ASCR, v.v.i., Boční II/1401, Prague 4, 14131, Czech Republic

[6] Géoazur, UMR 7329, CNRS, University of Nice - Sophia-Antipolis, 250 rue Albert Einstein, Valbonne Cedex, France

The role of magma in deformation and exhumation of deep orogenic crust is a matter of debate in many accretionary orogens. We use structural, petrological and geochronological observations to examine processes of exhumation of partially molten crust in the late Devonian-early Carboniferous Chandman dome in the Mongolian tract of the Central Asian Orogenic Belt. The dome is made of a high-grade core of granitoids and migmatites and a low-grade metamorphic envelope interpreted as different crustal levels. Its tectonic evolution can be divided into three main stages acting over a period of ~ 20 Ma. Horizontal fabric of partially molten rocks and granitoids

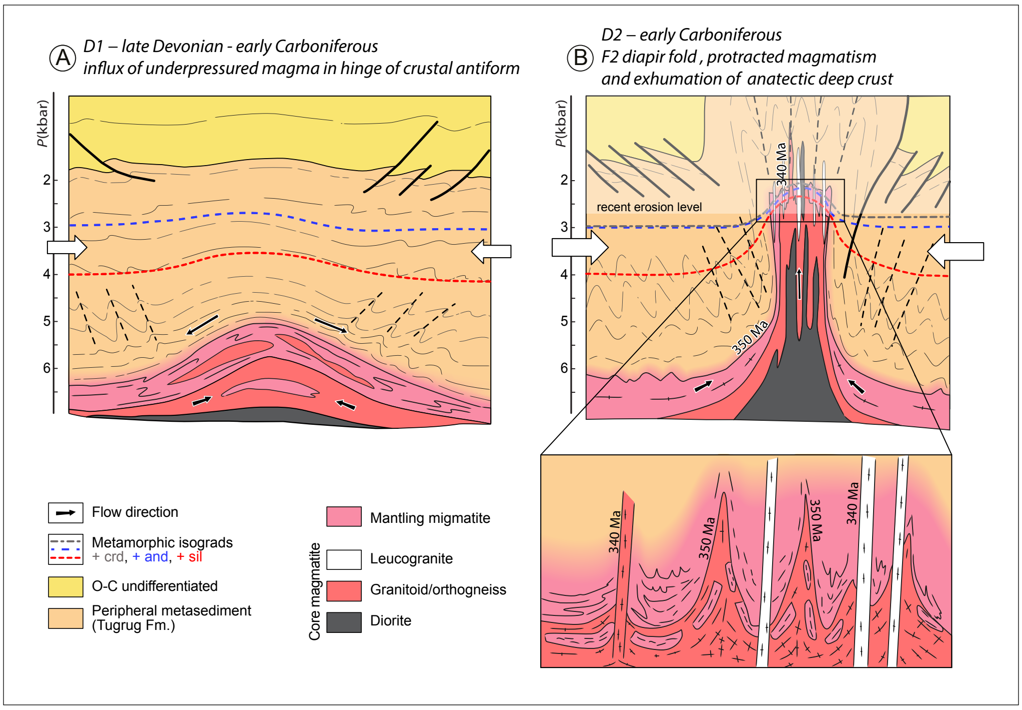

Figure 1. Idealized model of origin and evolution of the Chandman massif. (A) Initial stage showing onset of shortening in upper crustal levels and influx of partially molten crust into future fold core (similar to initiation of detachment fold of Bonini (2003), Fig. 12). (B) Final structure of the granite-migmatite dome characterized by vertically extruded partially molten crust and its juxtaposition to upper-crustal rocks. Lower inset shows cuspate-lobate geometry of migmatite and granitoid interface developed at ~ 350 Ma, and cross-cut by leucogranite dykes at ~ 340 Ma.

developed as a result of horizontal deep crustal flow at depth ~ 20 - 25 km. This stage was followed by upright folding associated with influx of partially molten crust into fold cores. Subsequent upward entrainment of these rocks was accommodated by magma-lubricated steep transfer zones coevally with isobaric heating of the surrounding upper crust at ~ 10 km. The dome formation is terminated by brittle expulsion of magma along vertical dykes parallel to upright fold axial planes during continuous cooling. We suggest that this tectonic evolution is analogous to the mechanical behavior of salt filling cores of detachment folds. In our model the fold core is initially filled by under-pressurized and buoyant magma that becomes rapidly overpressurized and extruded upwards as the fold locks-up similarly to salt diapirs in fold and-thrust belts. It is the continuous lateral shortening that triggers further vertical extrusion of buoyant magma along vertical dykes. In our view, detachment folding model explains well the lateral alternation of low-grade domains and migmatite magmatite zones commonly observed in accretionary orogens worldwide.

AN AGE FOR THE PILANESBERG COMPLEX, AND INSIGHT INTO ITS MANTLE ORIGIN: A PRELIMINARY REPORT.

Marlina Elburg

The age of the Pilanesberg Complex has long been a matter of controversy, with ages between 1100 and 1400 million years having been reported from various methods. In a new project addressing this problem as well as the petrogenesis and the origin of the magma, the new laser ablation multicollector inductively coupled plasma mass spectrometer (LA-MC-ICP-MS) that became operational in the beginning of 2916, has been utilized. While zircon is absent, titanite is sufficiently uranium-rich to provide a date, and multiple analyses allow the correction for common lead to be made automatically Fig. 2). Further, precise $^{87}Sr/^{86}Sr$ measurements made on the same instrument indicate magma provenance from a primitive (undepleted) mantle source (Fig. 3).

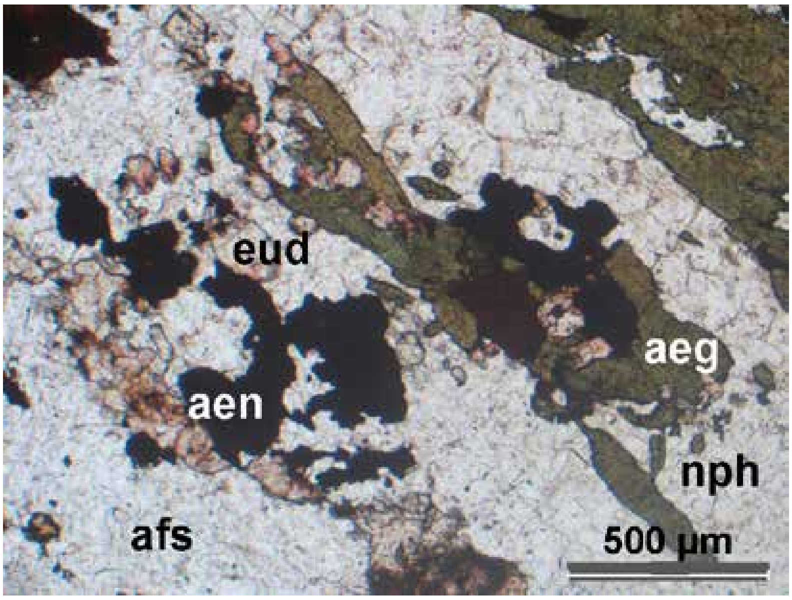

Figure 1. Thin section picture of sample of Green Foyaite, showing eudialyte, aenigmatite, aegirine, alkali-feldspar and nepheline.

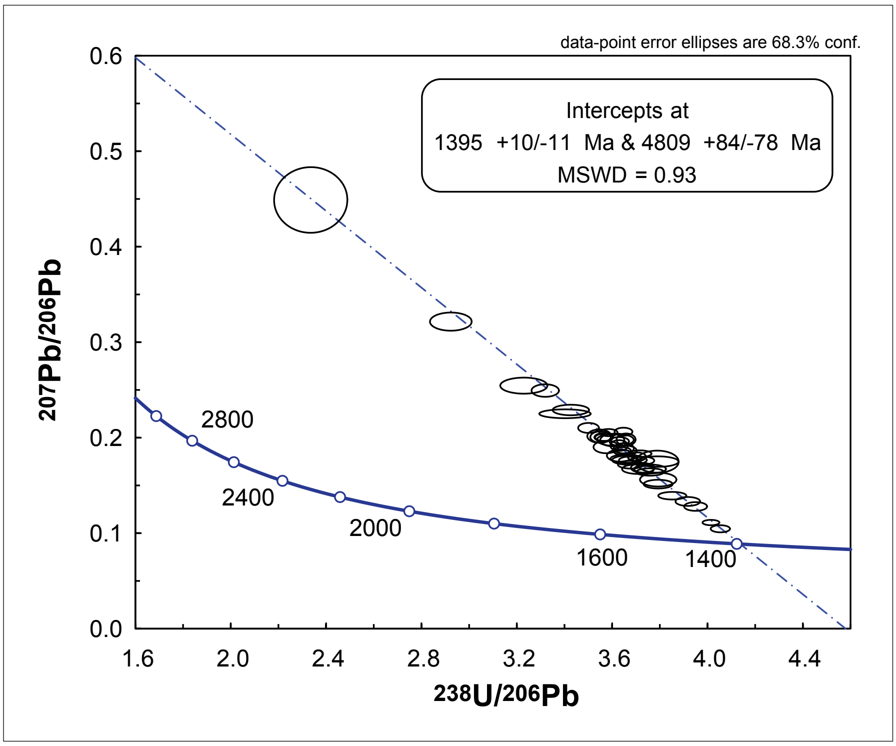

Figure 2. Tera-Wasserburg diagram for 43 in situ titanite U-Pb analyses from 5 samples of White Foyaite, obtained by LA-MC-ICPMS at the UJ Isotope Laboratory, housed in the Spectrum Analytical Facility.

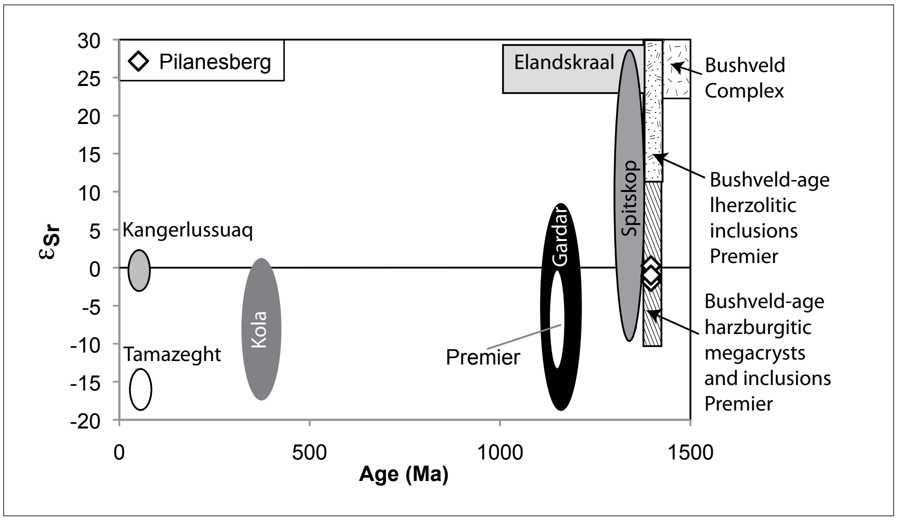

Figure 3. Sr isotopic ratio, expressed as epsilon Sr versus age for the Pilanesberg Complex, the local subcontinental lithospheric mantle and other alkaline complexes (literature data). The Pilanesberg Complex shows a signature of primitive mantle.

EARLY-MIDDLE JURASSIC MAFIC DYKES FROM THE H.U. SVERDRUPFJELLA, ANTARCTICA

Mabuela Morake, Mike Knoper, Geoff Grantham, Jan Kramers and Marlina Elburg

The Early to Middle Jurassic break-up of Gondwana produced large-volume magmatic events, resulting in large igneous provinces (LIPs) such as the Karoo LIP in southern Africa and Ferrar LIP in East Antarctica. The Early-Middle Jurassic mafic dykes from Sverdrupfjella located in western Dronning Maud Land (WDML), Antarctica, are regarded as part of the Karoo LIP [1]. These dykes intrude both the Grunehogna Province (an Archean basement fragment in WDML thought to have been a pre-breakup constituent of the Kalahari Craton) and the Maud Province (broadly co-eval with the Mesoproterozoic Namaqua-Natal metamorphic province in southern Africa). The dykes intruding the Grunehogna Province are considered on-craton, whereas those intruding the Maud Province are considered off-craton.

The geochemistry and geochronology of these dykes and basalts found in the Grunehogna Province and the Maud Province (Vestfjella, Heimefrontfjella and Kirwanveggen) have been studied by previous workers [e.g., 1) and have been categorized into two groups: low-Ti (TiO2 <2.5%) and high-Ti (TiO >2.5%) groups. Based on published ^{40}Ar/^{39}Ar ages of mafic dykes intruding the Grunehogna Province (on-craton), dyke emplacement occurred at ~178 Ma and ~190 Ma [1]. The Vestfjella basalts (off-craton) have K-Ar ages between 170-230Ma, and plagioclase K-Ar ages at ~180 Ma [2]. The Kirwanvergen basalts (off-craton) yielded a K-Ar age of 172 ± 10 Ma [3]. Mafic dykes in Sverdrupfjella that intrude Early Jurassic alkaline intrusive bodies (Straumsvola, Tvora and Jutulröra) show two ^{40}Ar/^{39}Ar age peaks: one at 178-175 Ma (Straumsvola) [4] and another at 206-204 Ma (Jutulröra) [5]. These dykes from the H.U. Sverdrupfjella are characterized by low TiO_2 and Zr contents. The dykes from Sverdrupfjella (off-craton) strike dominantly NNE-SSW, with dip angles ranging from 60° to 90°. The strike trends are similar to equivalent dykes from the on-craton region of WDML (Grunehogna Province, Almannryggen area) [1].

Samples collected from the Sverdrupfjella are fine to medium grained; the groundmass consists of plagioclase, augite and minor amounts of magnetite and ilmenite. Phenocrysts consist of plagioclase, olivine (with inclusions of Cr-spinel) and augite, and pseudomorphs of euhedral olivine and augite.

Unaltered dyke samples will be used for further age determination using ^{40}Ar/^{39}Ar data. Rb-Sr and Sm-Nd isotopic systematics will be used to evaluate mantle sources and crustal contamination. Initial ^{87}Sr/^{86}Sr ratios and Nd epsilon values of unaltered samples will be used to test models of derivation and petrogenesis. Isotopic ratios of ^{87}Sr/^{86}Srr ranging from 0.703361 to 0.711183, and ^{143}Nd/^{144}Nd180 epsilon values from 1 to -13 [6] would support derivation from heterogeneous mantle sources with melts affected by crustal contamination. Geochemical and geochronological data for the Early-Middle Jurassic dykes from Sverdrupfjella will be used to determine whether there is any overlap with similar data from the Karoo and Ferrar LIPs.

Figure 1. A Karoo-aged dyke intruding banded gneiss at Sverdrupfella.

References:

[1] Riley T.R. et al. (2005) Journal of Petrology 46:1489-1524.

[2] Luttinen A.V. and Furnes H. (2000) Journal of Petrology 41:1271-1305.

[3] Harris C. et al. (1990) Journal of Petrology 31(2): 341-369.

[4] Riley T.R et al. (2009) Mineralogical Magazine 73:205-226.

[5] Curtis M.L et al. (2008) Journal of Structural Geology 30:1429-1447.

[6] Grantham G.H. (unpubl. data)

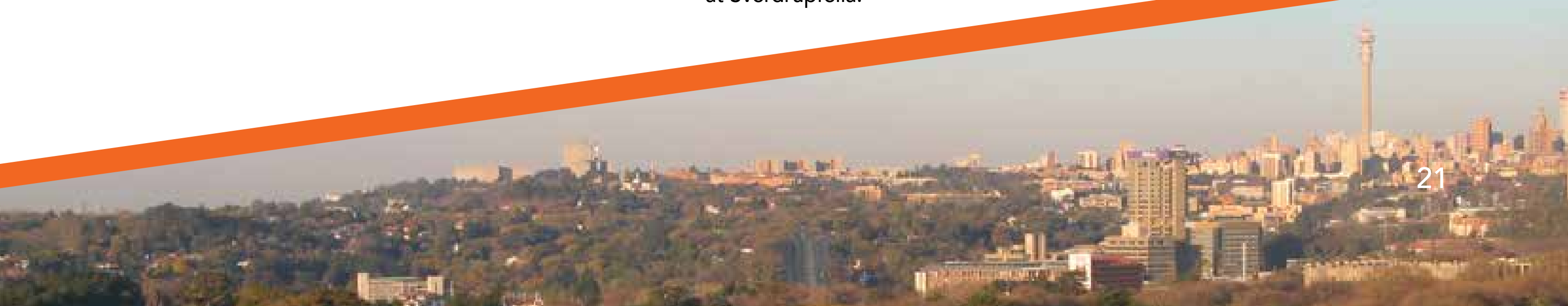

PRIMARY MAGMATIC AMPHIBOLE IN ARCHEAN META-PYROXENITE FROM THE CENTRAL ZONE OF THE LIMPOPO COMPLEX, SOUTH AFRICA

Georgy Belyanin[1], Mpho Keeditse[2], Mayuko Fukuyama[3], Toshiaki Tsunogae[4], HM Rajesh[2]

1 Department of Geology, University of Johannesburg, South Africa

2 Department of Earth and Environmental Sciences, BIUST, Botswana

3 Graduate School of Engineering and Resource Science, Akita University, Japan

4 Faculty of Life and Environmental Sciences, University of Tsukuba, Ibaraki, Japan

Although not widely reported, pyroxenites forming part of layered ultramafic to mafic intrusions are known from high-grade metamorphic terrains. Like other mafic and ultramafic members, pyroxenites generally occur as dismembered remains of the intrusion which was emplaced before the high-grade metamorphic event(s). In spite of the overprint events, these ultramafic intrusions often preserve the igneous minerals (e.g., olivine, orthopyroxene, clinopyroxene) in a granoblastic polygonal textured framework. On the other hand, metamorphic minerals (e.g., amphibole, garnet), formed during the overprint event(s), commonly exhibit textural relations indicative of their formation after the igneous minerals. In the less common scenario, the meta-pyroxenites are characterized by granoblastic re-equilibration textures with 120° triple junction between the prominent minerals, with no new metamorphic mineral formed during the overprint event(s).

Reports on the occurrence of primary amphiboles from the high-grade metamorphosed rock units, especially the earlier ultramafic rocks, of a layered intrusion are rare; the only available

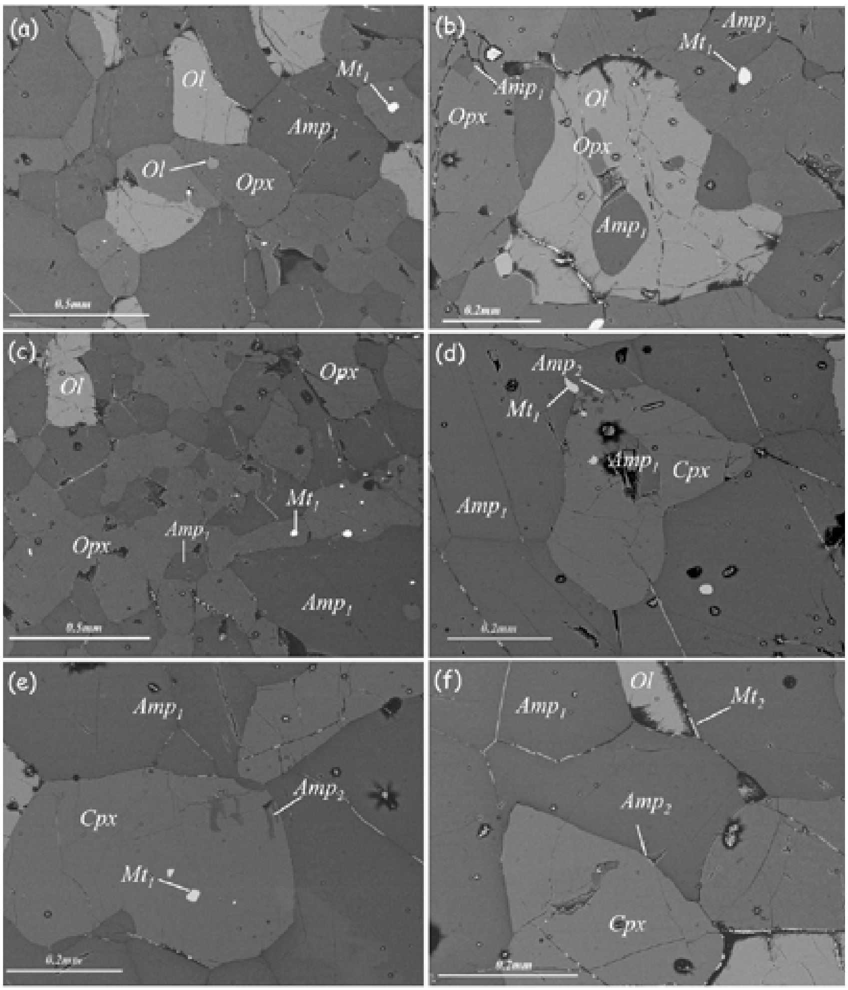

Figure 1. Representative BSE images illustrating the relation between the various rock forming minerals in the Sand River meta-pyroxenite. Amp_1 – primary amphibole; Amp_2– secondary amphibole; Mt_1– primary magnetite; Mt_2 – secondary magnetite.

reports are from the Archean (~2.97 Ga) Fiskenæsset layered complex in *southwestern Greenland* (Polat et al., 2012). Here we describe another example of primary magmatic amphibole. It was found in a meta-pyroxenite from the Musina layered intrusion occurring within the high-grade metamorphic Central Zone of the Limpopo Complex in South Africa. Considering the poly-metamorphic nature of the study area, detailed petrographic characterization aided with a scanning electron microscope (SEM) was used to understand the mutual relation between the different rock forming minerals, including amphibole, and the effect of metamorphic overprint events.

The Central Zone of the Limpopo Complex is comprised of a variety of deformed supracrustal rocks (Beit Bridge Complex, with detrital zircons of >3.8 Ga) and minor mafic to ultramafic rocks (~3.35 Ga Musina layered intrusion), which are tectonically interleaved within voluminous granitoid orthogneisses (~3·31-3·28 Ga migmatitic Sand River TTG gneisses, and various ~2·73-2·60 Ga granitoid gneisses) [*Smit et al.*, 2011]. The latter Paleoproterozoic tectono-metamorphic event (~2.0 Ga) is related to the formation of anatectic intrusions and granitic pegmatites as well as reactivation along shear zones. The meta-pyroxenite reported here forms part of the Musina layered intrusion. Both mafic (gabbro) and ultramafic (pyroxenite-peridotite) rocks of the intrusion occur as conformable layers in migmatitic metapelitic gneiss in the mapped Sand River section.

The studied sample of meta-pyroxenite shows a uniform granoblastic-polygonal texture, and is made up of amphibole (up to 40% modal proportion), clinopyroxene (~25%), orthopyroxene (~20%), and olivine (~10%), with minor magnetite (~3%), apatite, pyrite and pentlandite. In terms of modal proportions, it is an amphibole websterite. The main minerals – olivine, clinopyroxene, orthopyroxene and amphibole – occur as subhedral to anhedral grains. In terms of inclusion-host relation, rare rounded olivine was observed within orthopyroxene (Fig. 1a), rare rounded orthopyroxene – within olivine, clinopyroxene and amphibole (Fig. 1b), and amphibole inclusions (with straight or rounded outline) – within orthopyroxene, clinopyroxene and olivine (Figs. 1b, c and d). In addition to the dominant variety (Amp_1), occurring as polygonal grains as well as inclusions, a second variety of amphibole (Amp_2) occurs in the meta-pyroxenite. Amp_2 dominantly occurs as small grains replacing clinopyroxene adjacent to grain margins (Figs. 1d and e). They also occur as thin rims between clinopyroxene and Amp_1 (Fig. 1f), and as rare interstitial grains surrounded by larger Amp_1 grains or between clinopyroxene and Amp_1 grains. Surprisingly, alteration is minimal in the rock and, in spite of obvious metamorphic re-equilibration, no new metamorphic mineral was observed.

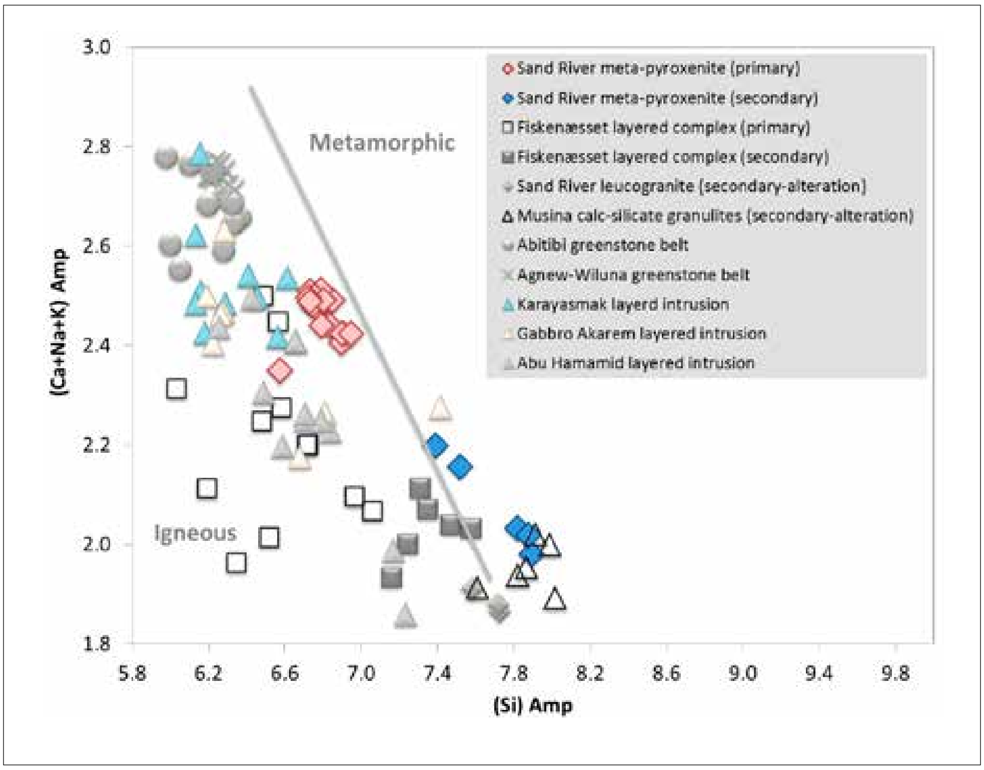

Figure 2. Ca+Na+K (apfu) versus Si (apfu) mineral chemistry based diagram evaluating the primary versus secondary trend of amphiboles in the Sand River meta-pyroxenite.

Based on their petrographic features and trends in Fig. 2 we suggest that the amphiboles occurring as inclusions and polygonal grains in the Sand River meta-pyroxenite are primary magmatic. But their compositions consistently fall at a slightly different position with respect to all magmatic amphiboles compared in figure 2, indicating the effect of metamorphic re-equilibration. Thus, our identification of primary magmatic amphiboles in meta-pyroxenites, part of the Archean Musina layered intrusion, implies hydrous conditions in the Archean. Like the scenario of the *Müntener et al.* (2011) experiments, which simulated natural, arc magma compositions, possible derivation in a H_2O-rich subduction setting cannot be discounted as an analogue for the formation of Archean layered intrusions and this needs to be tested by future studies.

Müntener, O., Kelemen, P.B., Grove, T.L., 2001. The role of H_2O during crystallization of primitive arc magmas under uppermost mantle conditions and genesis of igneous pyroxenites: an experimental study. Contributions to Mineralogy and Petrology, 141, 643-658.

Polat, A., Fryer, B.J., Samson, I.M., Weisener, C., Peter, W.U., Frei, A.R., Windley, B.F., 2012. Geochemistry of ultramafic rocks and hornblendite veins in the Fiskenæsset layered anorthosite complex, SW Greenland: Evidence for hydrous upper mantle in the Archean. Precambrian Research, 214-215, 124-153.

Smit, C.A., Van Reenen, D.D., Roering, C., Boshoff, R., Perchuk, L.L., 2011. Neoarchean to Paleoproterozoic evolution of the polymetamorphic Central Zone of the Limpopo Complex. Geological Society of America Memoir, 207, 213-244.

Mineralogy

GEOCHEMICAL CHARACTERISTICS OF BERYL FROM PEGMATITES OF THE ERONGO VOLCANIC COMPLEX, NAMIBIA

Julieta Lum, Fanus Viljoen and Bruce Cairncross

The granite-hosted pegmatites of the Erongo Volcanic Complex in central Namibia are well known for the occurrence of a number of mineral types, of much interest to collectors. A variety of beryl types with colours ranging from green, yellow (heliodor), colorless (goshenite) and blue/greenish blue (aquamarine) are found in miarolitic cavities within the pegmatites. This contribution serves to document and discuss their phyical appearance, inclusion content, and their major and trace element chemistry. To this end, 25 blue beryls, as well as two green beryls and one colourless beryl were investigated using SEM, EMPA and LA-ICP-MS in order to gain insight into chemical differences between the various beryl types, their chromophores, and their similarities or differences to other beryls worldwide. The beryls from Erongo are generally subhedral to euhedral with a well-formed prismatic habit. Idiomorphic crystals, characterized by well developed hexagonal prisms, are

Fig. 1 Pale aquamarine from Erongo

common. Common associated minerals include schorl, quartz, muscovite, alkali feldspar, plagioclase feldspar, iron oxides, foitite, rossmanite and cassiterite.

Aquamarines range from pale blue to deep blue, or greenish blue, with pronounced colour zoning. The two green specimens vary in colour from pale green to pale greenish yellow. Levels of transparancy vary. One green beryl is medium green and heavily included whereas the other specimen has a pale yellowish green colour. Transparency is heavily influenced by cracks, often filled with secondary iron oxides. Mineral inclusions are common and include schorl, quartz, muscovite, feldspar, iron oxides and cassiterite, clearly reflective of the host pegmatite mineralogy.

Aquamarine and green beryl contain iron as the main chromophore while goshenite is devoid of chromophores. Increasing colour saturation correlates with increasing Fe, consistent with the known chromatic effects of Fe in blue, yellow and green beryl. Although optically and chemically homogeneous specimnes are common, colour-zoned, optically heterogeneous crystals are also encountered. These are characterised by variable Fe_{tot} (0.79-3.19 wt% FeO), Na (0.09-0.35 wt% Na_2O), and Al (15.99-18.18 wt% Al_2O_3). Zoning patterns range from simple core-to-rim transitions to more complex sector and/or oscillatory zoning, with chemical trends which correspond to previously documented substitutions for beryl worldwide.

Octahedral cation substitution is the dominant mechanism for the incorporation of a variety of minor and trace elements, e.g. Na, which is mainly incorporated (over Cs) at the channels (to maintain charge balance). Based on charge balance arguments, some tetrahedral Be-Li substitution is also indicated. Trace element concentrations, as determined through LA-ICP-MS analysis, are variable, with highest concentrations encountered in the aquamarines. Cs, Sc, Ga and Mn are positively correlated with Rb, consistent with the incorporation of these elements at the octahedral site (Sc, Mn and minor Ga) or the channel site (Cs, Rb), in order to preserve charge balance. In contrast, Ca, Zn and Ti do not correlate with Rb, nor with Cs. This is unexpected, as Ti and Ca are known to substitute at the octahedral site in beryl, while Ca may also enter the 2a channel site. Consistently low Cr contents in all the samples examined concur with Cr not being a chromophore element for the green beryl examined in the present study. Overall, major and trace element contents are similar to those of other beryls (aquamarines) worldwide, with no distinctive locality-specific chemistries observed, when compared to the worldwide database.

Subrecent and Medical Geology

INVESTIGATING GEOGENIC LEAD CONTAMINATION AND ITS EFFECTS ON HEALTH IN THE KILIFI AREA, KENYA

Christa Koki[1], Hassina Mouri[1] and L. Olaka[2]

[1] Department of Geology, University of Johannesburg - APK, South Africa

[2] Department of Geology, University of Nairobi, Chiromo Campus, Kenya

According to WHO, lead (Pb) toxicity accounts for 0.6% of the global disease burden [7]. Humans are exposed through food, water and air. Prolonged exposure affects the nervous, immune among other body systems [2]. Children are more susceptible to its poisoning with a potential damage to the normal brain development [2, 8]. Anthropogenic activities and geogenic sources release it to the environment. In the Kilifi area (Fig. 1), sedimentary rocks of Triassic to Recent age host a base metal deposit of galena [3]. This area was heavily mined in the 1970s and the un-rehabilitated mines remain, exposing rock tailings to weathering agents [4]. Chronic diseases such as rheumatism, anaemia and neuro-developmental disorders for instance intellectual disability and epilepsy that have been associated to heavy metal contamination in other parts of the world have been reported in this area too [1, 5, 8]. A study conducted in 2013 shows that 7.8/1000 people have Active Convulsive Epilepsy with children being highly affected [6]. Since lead toxicity is also known to cause brain disorders, cardiovascular effects and nephrotoxicity in kidneys, it is important to investigate the relationship between geology and disease prevalence in the Kilifi area. This is crucial simply because, over 70% of the locals live below 2 USD per day relying on the natural resources and are mainly subsistence farmers. Notably, the study area comprises of a health surveillance system (Kilifi Demographic and Health Surveillance System KDHSS– Fig. 2), an area about 891Km2, which was established in 2000 and is made up of 15 locations. The KDHSS database comprises a record of births, pregnancies, migration events and deaths. It is maintained by 4 monthly household visits and has geographical boundaries set with reference to the areas served by the Kilifi District Hospital (KDH) which is the only in-patient facility offering pediatric services. This study aims at investigating the vulnerability of the Kilifi residents to geogenic lead contamination through analysing soil, water and food crop samples for lead, correlating the analysis results with health data on chronic diseases associated with lead/heavy metal contamination and producing spatial correlation maps.

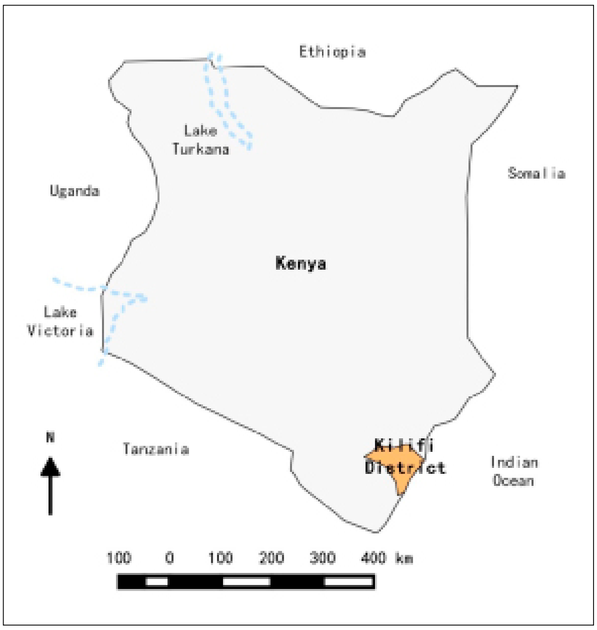

Figure 1. Map of Kenya showing the Kilifi District

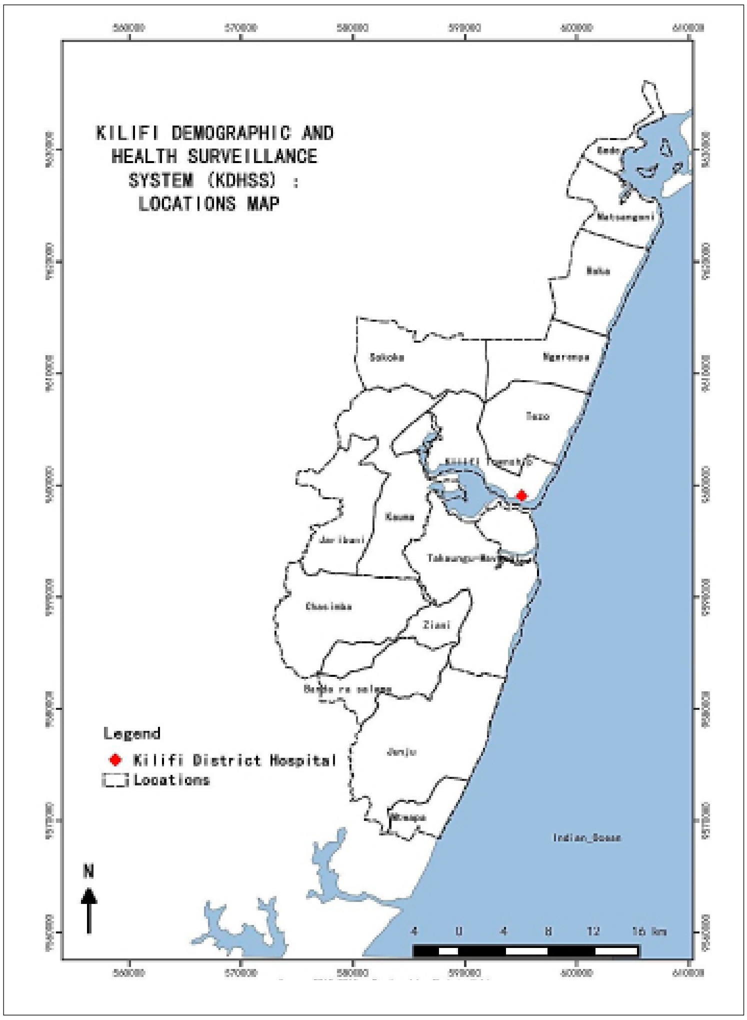

Figure 2. Kilifi Demographic and Health Surveillance System (KDHSS) map

References:

[1] Alam M.G et al. (2003) Sci Total Environ 308:83-96

[2] Ali S.M et al. (2011) Environ Polln 20: Springer Sci and Business Media B.V

[3] Caswell P.V (1956) Geol of Kilifi-Mazeras No 34 Geol. Surv. Kenya

[4] Horkel A.D et al. (1984) Geol and Min Res of the Southern Kenyan Coast. Geol. Surv. 151-159

[5] Newton C. R and Garcia H (2012) Lancet. 380:1193-1201

[6] Ngugi A.C et al. (2013) Lancet Neuro – Elsevier

[7] World Health Organization (2010) Childhood Lead Poisoning WHO Library, 1-74

[8] Von Schirnding Y et al. (2003) Environ Res. 93(3):259-263.

(U-TH)/HE DATING OF $CACO_3$ SPELEOTHEMS: A NEW PERSPECTIVE FOR DATING FOSSIL-BEARING CAVE DEPOSITS

Tebogo V. Makhubela and Jan D. Kramers

Cave mapping and geological studies in the Cradle of Humankind (CoH) site have revealed that 81 caves contain evidence of macrofossils and 15 are known to contain hominin or archaeological remains from a variety of ages between 0 and 3 Ma [1]. Deposits of the CoH have been traditionally dated on the basis of biostratigraphic correlation [2], and in spite of recent advances particularly in U-Pb dating, dating many fossil-bearing deposits older than the c. 0.5 Ma limit for U-Th dating remains a challenge [3,4].

(U,Th)-He dating of fossil aragonites was first carried out in 1965 [5]. Although the method is used routinely for apatite thermochronology, retention of He in calcite was first demonstrated in 2007 [6] and the first successful dating of a fault-filling calcite in 2014 [6]. Given retention of He, the (U,Th)-He dating offers some potential advantages over (U,Th)-Pb. First, sensitivity, because many more nuclides are produced in the course of decay (8 for ^{238}U, 7 for ^{235}U and 6 for ^{232}Th), and second, absence of initially built-in He in samples. In this study we have explored the dating of calcium carbonate flowstones, interbedded with fossil-bearing breccia deposits at the CoH, using this dating technique. Sample powders or grains, wrapped in copper foil, were heated using a laser to analyze helium using a ^{3}He spike, after which the sample is removed from the vacuum chamber, dissolved and analysed for U and Th by isotope dilution. For laser heating, a continuous 1064 nm Nd-YAG laser was used which necessitated carbon coating of the foil package (Fig. 1). Challenges are the large release of CO2 (captured on cold traps) and sometimes hydrocarbons that impede He ionization, as well as quantitative recovery of samples after degassing. The method was tested on well-dated flowstone samples from Swartkrans, where we have reproduced within error an age of 1.8 Ma for a sample dated to 1.816 ± 0.041 Ma using U-Pb [8] and which relates to clastic sediments in member 1 for which a similar age (1.80 ± 0.09 Ma) has been obtained using cosmogenic nuclides burial dating [9]. This and other preliminary results show that the method is promising as a technique that might help radiometrically date fossil-bearing cave deposits of the CoH.

Further development will include constructing a small oven, which will make it possible to analyse larger samples (up to about 100 mg) than is possible using a laser, thus making it possible to carry out (U,Th) disequilibrium analyses on samples after helium extraction.

Figure 1. samples encapsulated in copper foil and carbon coated. Internal sample holder diameter is 3 mm.

References:

[1] Dirks PHGM and Berger LR (2013) Journal of African Earth Sciences 78: 109-131

[2] Berger LR, Lacruz R and de Ruiter DJ (2002) American Journal of Physical Anthropology 119: 192-197

[3] Herries AIR, Curnoe D and Adams JW (2009) Quaternary International 202: 14–28

[4] Bruxelles L, Clarke RJ, Maire R, Ortega R and Stratford D (2014) Journal of human evolution 70: 36–48

[5] Fanale FP and O. A. Schaeffer, OA (1965) Science 149, 312-317

[6] Copeland P, Watson EB, Urizar SC, Patterson D and Lapen TJ (2007) Geochimica et Cosmochimica Acta 71: 4488–4511

[7] Cros A, Gautheron C, Pagel M, Berthet M, Tassan-Got L, Douville E, Pinna-Jamme R and Sarda P (2014) Geochimica et Cosmochimica Acta 125: 414-432

[8] Pickering R, Kramers JD, Hancox PJ, De Ruiter DJ and Woodhead JD (2011) Earth and Planetary Science Letters 306: 23–32

[9] Gibbons RJ, Pickering TR, Sutton MB, Heaton JL, Kuman K, Clarke RJ, Brain CK and Granger DE (2014) Quaternary Geochronology 24: 10-1524

POSTGRADUATE STUDENTS IN PPM (2015)

STUDENT	P/F time	THESIS TOPIC	SUPERVISORS
Adeniyi, Elijah (MSc)	F	Gas potential in Karoo (Karen project)	N. Beukes
Boshoff, Pedro (MSc)	P	Speleogenesis in Cradle of Humankind	J. Kramers, H. van Niekerk
Bukanga, Amuli (MSc)	P	Small scale mining, olivine	F. Senzani
De Kock, Conrad (MSc)	F	Mineralization at Sishen iron mine	A.J.B. Smith, N.J. Beukes
De Villiers, Mike (MSc)	P	African Rift volcanics	H. Mouri
Fabien, Francis (MSc)	P	Coal oxidation in underground mines	N. Wagner
Fitschen, Juergen (MSc)	P	Stress-strain analysis, Barberton M.L.	A. Hofmann
Fitzpatrick, Stuart (MSc)	F	Palaeomagnetism, continent reconstruction	M.O. de Kock, H. van Niekerk
Gevera, Patrick (MSc)	F	Medical Geology	H. Mouri
Hlongwani, Caroline (MSc)	F	Study of iron mineralization	A.J.B. Smith
Kekana, Papi (MSc)	F	Temporal and spatial variation coal quality	N. Wagner
Koki, Christa (MSc)	F	Medical Geology	H. Mouri
Magwaza, Boniswa (MSc)	F	Zircons in metamorphism	M. Elburg
Masangane, Noma (MSc)	F	Iron mineralization, Wolhaarkop Dome	A.J.B. Smith, N.J. Beukes
Mashamba, M. Lucas (MSc)	P	Acid mine drainage, Brugspruit, MP	J. Kramers, H. Coetzee (CGS)
Matiane, Arnold (MSc)	F	Rare Earth Elements in coal ashes	N. Wagner
Mgoqi, Aviwe (MSc)	F	Acid rock drainage, MP and Limpopo	J. Kramers, D. Love (Golder assoc.)
Moitsi, Ernest (MSc)	F	Geometallurgy, Merensky reef	K.S. Viljoen, M. Knoper
Monareng, Fisah (MSc)	F	Paleomagnetism, Kalahari Manganese Field	M.O. de Kock, N. Beukes, L. Blignaut
Morake, Mabuela (MSc)	F	Karoo-related dykes in Antarctica	M. Knoper, M. Elburg, J. Kramers
Mpanza, Zama (MSc)	F	Cratonic mantle beneath Premier kimberlite	K.S. Viljoen
Mphaphuli, Maseda (MSc)	F	Soutpansberg Coalfield	N. Wagner
Naude, Grethe (MSc)	P	Process temperature in a semi-coke plant	N. Wagner
Nendouvhada, Ndivhuho (MSc)	F	Comparison coal composition in Botswana	N. Wagner
Ndhlovu, Brian (MSc)	F	Geometallurgy of sulphides in the Plat Reef	K.S. Viljoen
Nkomo, Thobeka (MSc)	F	Pb-Zn-Cu ores of Aggeneys-Gamsberg	K.S. Viljoen
Nthloro, Boitumela (MSc)	F	Iron mineralization Kolomela Mine	A.J.B. Smith, N. Beukes
Opperman, Alicia (MSc)	P	Structural geology, Kalahari Mn field	N.J. Beukes, L.C. Blignaut

Radzivhoni, Charles (MSc)	P	Geometallurgy Mogalakwena Mine	K.S. Viljoen
Rammilla, Ephriam (MSc)	F	Izermyn iron formation, Sinqeni Fm.	N.J. Beukes, A.J.B. Smith
Ravhura, Livhuwani (MSc)	F	Geochronology of Molopo Farms Complex	N.J. Beukes, C. Vorster, M.O. de Kock
Terblanche, Sullivan (MSc)	F	Geomorphology of Buffalo River Catchment	H. van Niekerk
Tsunke, Mpho (MSc)	P	Sethlabotse project, Highveld coalfield	B. Cairncross
Vafeas, Nic (MSc)	F	Metallogeny of low grade Mn ores	N. Beukes, M. de Kock
Zardad, Sabiyya (MSc)	F	Geometallurgy of manganese ore	A.J.B. Smith, K.S. Viljoen
Blignaut, Lauren (PhD)	P	Ore genesis in Manganese Fields	K.S. Viljoen, H. Tsikos
Chabalala, Vongani (PhD)	P	Coal petrology applied to gas exploration	N. Wagner
Dzvinamurungu, Thomas (PhD)	F	Metallogenesis of Nkomati nickel mine	K.S. Viljoen
Lum, Jullieta (MSc)	F	Beryl minerals of Southern Africa	K.S. Viljoen, B. Cairncross
Luskin, Casey (PhD)	F	Palaeomagnetic studies	M. de Kock
Makhubela, Tebogo V. (PhD)	P	Geochronology of cave deposits, landscape evolution	J. Kramers, D. Scherler, G. Belyanin
Mkhatshwa, Sindile (PhD)	F	Geometallurgical studies	K.S. Viljoen
Nxumalo, Valerie (PhD)	P	Springbok Flats Coalfield, uranium and sediment provenance	J. Kramers, B. Cairncross, C. Vorster
Rose, Derek (PhD)	P	Geometallurgy of PGE ore at two Rivers	K.S. Viljoen. H. Mouri
Singo, N. Kenneth (PhD)	P	Remediation of abandoned mines	J. Kramers
Vieira da Costa, Giuliana (PhD)	F	Studies of Archean sedimentary environment	A. Hofmann

POSTDOCTORAL ASSOCIATES IN PPM (2015)

Dongre, Ashish
Geochemical studies of kimberlites

Eickmann, Benjamin
Mineralogy, geochemistry and isotope studies related to the environment of early life

Gucsik, Arnold
Shock phenomena, cosmology and general applications of Raman spectroscopy

Humbert, Fabien
Structural and paleomagnetic studies on the Paleoproterozoic Hekpoort and Ongeluk volcanic formations, and implications for the evolution of the Transvaal Basin

Ossa Ossa, Frantz Gerard
Mineralogical and geochemical studies of low grade metamorphism and diagenesis, particularly related to uranium mineralization

MSc and PhD STUDENTS THAT GRADUATED IN 2015

Dlamini, Ntombifuthi (MSc)
Geochemical and geochronological studies of Archean rock units in southern Swaziland

Makhubela, Tebogo V. (MSc., cum laude)
^{40}Ar/^{39}Ar and (U,Th)-He dating attempts on the fossil-bearing cave deposits of the Malapa and Sterkfontein hominin sites of the Cradle of Humankind, South Africa

Pienaar, Donovan (MSc)
A Geometallurgical Characterization of the Vaal Reef-A Facies at Moab Khotsong Mine, AngloGold Ashanti, with specific focus on Gold and Uranium deportment

Turnbull, Sara Jane (MSc)
Petrography, Mineral Chemistry and Ar-Ar Isotope characteristics of the Ledig Lujavrites, on the SW edge of the Pilanesberg Complex

Fraser, Allan W. (MSc)
Improvements in analytical techniques relating to ore assessment

Maré, Leonie P. (PhD.)
Geothermal history of theKaroo Basin in South Africa inferred from magnetic studies

McLoughlin, A.C. (MSc)
A Geometallurgical Examination of Gold, Uranium and Thorium in the Black Reef Quartzite Formation

Munyangane, P. (MSc)
Medical Geology in the Giyani area

Pretorius, Donavan (MSc)
Mineralogical assessment of coal from the New Vaal colliery through the application of automated mineralogy, with a view on possible benificiation

PUBLISHED PAPERS, 2015 (peer-reviewed international journals)

Agangi A, Hofmann A, Kamenetsky VS, Vroon PZ (2015). Paleoarchean felsic magmatism: a melt inclusion study of 3.45 Ga old rhyolites from the Barberton Greenstone Belt, South Africa. Chemical Geology 414, 69-83.

Agangi, A., Hofmann, A., Rollion-Bard, C., Marin-Carbonne, J., Cavalazzi, B., Large, R., Meffre, S., (2015). Gold accumulation in the Neoarchean Witwatersrand Basin, South Africa – evidence from concentrically laminated pyrite. Earth-Science Reviews 140, 27-53.

Agangi, A., Przybyłowicz, W., Hofmann, A. (2015). Trace element mapping of pyrite from Archean gold deposits–A comparison between PIXE and EPMA. Nuclear Instruments and Methods in Physics Research Section B: Beam Interactions with Materials and Atoms 348, 302-306.

Andreoli, M.A.G., Przybylowicz, W.J., Kramers, J., Belyanin, G., Westraadt, J., Bamford, M., Mesjasz-Przybylowicz, J., b, A. Venter, A., 2015. PIXE micro-mapping of minor elements in Hypatia, a diamond bearing carbonaceous stone from the Libyan Desert Glass area, Egypt: Inheritance from a cold molecular cloud? Nuclear Instruments and Methods in Physics Research B, 363, 79-85.

Aulbach S, Viljoen KS (2015) Eclogite xenoliths from the Lace kimberlite, Kaapvaal craton: From convecting mantle source to palaeo-ocean floor and back. Earth and Planetary Science Letters 431 : 274-286.

Avice, G., Meier, M.M.M., Marty, B., Rainer Wieler, R., Kramers, J.D., Langenhorst, F., Cartigny, P., Maden, C., Zimmermann, L., Andreoli, M.A.G., 2015. A comprehensive study of noble gases and nitrogen in "Hypatia", a diamond-rich pebble from SW Egypt. Earth Planet. Sci. Lett., 432, 243–253

Bolhar, R., Hofmann, A., Siahi, M., Feng, Y. X., and Delvigne, C. (2015). A trace element and Pb isotopic investigation into the provenance and deposition of stromatolitic carbonates, ironstones and associated shales of the ~3.0 Ga Pongola Supergroup, Kaapvaal Craton. Geochimica et Cosmochimica Acta 158, 57-78.

Bons, P.D., Baur, A., Elburg, M.A., Lindhuber, M.J., Marks, M.A.W., Soesoo, A., van Milligen, B.P., Walte, N.P. (2015). Layered intrusions and traffic jams. Geology 43, 71-74.

Broussolle, A., Štípská, P., Lehmann, J., Schulmann, K., Hacker, B.R., Holder, R., Kylander-Clark, A.R.C., Hanžl, P., Racek, M., Hasalová, P., Lexa, O., Hrdličková, K., Buránek, D. 2015. P–T–t–D record of crustal-scale horizontal flow and magma-assisted doming in the SW Mongolian Altai, Journal of Metamorphic Geology, 33(4), 359–383, doi: 10.1111/jmg.12124.

Chitsiga T.L, Daramola, M.O., Wagner N.J., Ngoy, J.M. (2015). Effect of the presence of water-soluble amines on the Carbon Dioxide (CO_2) adsorption capacity of amine-grafted poly-succinimide (PSI) adsorbent during CO_2 Capture. Energy Procedia 86, p 90 - 105.

Dai, S., Wang, P., Ward C.R., Tang, Y., Song, X., Jiang, J., Hower, J.C., Li, T., Seredin, V.V., Wagner, N., Jiang, Y., Wang, X., Liu, J. 2015. Elemental and mineralogical anomalies in the coal-hosted Ge ore deposit of Lincang, Yunnan, southwestern China: Key role of N_2-CO_2-mixed hydrothermal solutions. International Journal of Coal Geology. Vol 152 19-46

de Kock, M.O., Beukes, N.J., and Mukhopadhyay, J., 2015. Palaeomagnetism of Mesoproterozoic limestone and shale successions of some Purana basins in southern India. Geological Magazine, 152: 728-750

Dindarloo, S.R., Bagherieh, A., Hower, J.C., Calder, J.H., Wagner N.J. 2015. Coal modeling using Markov Chain and Monte Carlo simulation: Analysis of microlithotype and lithotype succession. Sedimentary Geology 329 (1-11).

Dirks, P.H.G.M., Berger, L.R., Roberts, E.M., Kramers, J.D., Hawks, J., Randolph-Quinney, P.S., et al., 2015. Geological and taphonomic context for the new hominin species Homo naledi from the Dinaledi Chamber, South Africa. eLIFE, 2015;4:e09561. DOI: 10.7554/eLife.09561, 37pp

Dongre AN, Jacob DE, Stern RA (2015) Subduction-related origin of eclogite xenoliths from the Wajrakarur kimberlite field, Eastern Dharwar craton, Southern India: Constraints from petrology and geochemistry. Geochimica et Cosmochimica Acta 166 : 165-188.

Dongre AN, Viljoen KS, Malandkar M (2015) The Pipe-15 kimberlite: A new addition to the Wajrakarur cluster of the Wajrakarur kimberlite field, Eastern Dharwar Craton, southern India. Journal of the Geological Society of India 86 : 71-79.

Elburg, M., Jacobs, J., Andersen, T., Clark, C., Läufer, A., Ruppel, A., Krohne, N., Damaske, D. (2015). Early Neoproterozoic metagabbro-tonalite-trondhjemite of Sør Rondane (East Antarctica): Implications for supercontinent assembly. Precambrian Research 259, 189-206.

Farber K, Dziggel A, Meyer FM, Prochaska W, Hofmann A, Harris C (2015). Fluid inclusion analysis of silicified Palaeoarchaean oceanic crust - a record of Archaean seawater? Precambrian Research 266, 150-164.

Franchi F, Hofmann A, Cavalazzi B, Wilson A, Barbieri R, (2015). Determining marine vs hydrothermal influences in Devonian carbonate mounds using rare earth elements (Kess Kess mounds, Anti-Atlas, Morocco). Chemical Geology 409, 69-86.

Gumsley, A., Olsson, J., Soderlund, U., de Kock, M., Hofmann, A. and Klausen, M., 2015. Precise U/Pb baddeleyite age dating of the Usushwana Complex, southern Africa; implications for the Mesoarchaean magmatic and sedimentological evolution of the Pongola Supergroup, Kaapvaal Craton. Precambrian Research, 267: 174-185

Hicks, N., Elburg, M., Andersen T. (2015). U-Pb and Hf isotope constraints for emplacement of the Nkandla Granite, southeastern Kaapvaal Craton, South Africa. South African Journal of Geology 118 (2), 119-128.

Hofmann, A., Kröner, A., Xie, H., Hegner, E., Belyanin, G., Kramers, J., Bolhar, R., Slabunov, A., Reinhardt, J., Horváth, P. (2015). The Nhlangano gneiss dome in south-west Swaziland - a record of crustal destabilization of the eastern Kaapvaal craton in the Neoarchaean. Precambrian Research 258, 109–132.

Hofmann, A., Mazumder, R. (2015). A review of the current status of the Older Metamorphic Group and Older Metamorphic Tonalite Gneiss: insight into the Palaeoarchean history of the Singhbhum craton, India. In: Mazumder, R. & Eriksson, P. G. (eds) Precambrian Basins of India: Stratigraphic and Tectonic Context. Geological Society, London, Memoirs, 43, 103–107, http://dx.doi.org/10.1144/M43.7

Jacobs, J., Elburg., M., Laeufer, A., Kleinhanns, I.C., Henjes-Kunst, F., Estrada, S., Ruppel, A., Damaske, D., Montero, P., Bea, F. (2015). Two distinct Late Mesoproterozoic/Early Neoproterozoic basement provinces in central/eastern Dronning Maud Land, East Antarctica: the missing link, 15-21°E. Precambrian Research 265, 249-272.

Koegelenberg, C., Kisters, A.F.M., Kramers, J.D., Frei, D., 2015. U–Pb detrital zircon and ^{39}Ar–^{40}Ar muscovite ages from the eastern parts of the Karagwe-Ankole Belt: Tracking Paleoproterozoic basin formation and Mesoproterozoic crustal amalgamation along the western margin of the Tanzania Craton. Precambrian Research, 269, 147-161.

Lehmann, J., Master, S., Rankin, W., Milani, L., Kinnaird, J.A., Naydenov, K.V., Saalmann, K., Kumar, M. 2015. Regional aeromagnetic and stratigraphic correlations of the Kalahari Copperbelt in Namibia and Botswana, Ore Geology Reviews, 71, 169-190, doi:10.1016/j.oregeorev.2015.05.009.

Mavhengere, P., Maphala, T., Wagner, NJ. 2015. Physical and Structural Effects of Carbon Dioxide Storage on Vitrinite-Rich Coal Particles Under Supercritical and Subcritical Conditions. International Journal of Coal Geology: 150–151 (1–6).

Mavhengere, P., Vittee, T., Wagner, NJ., Kauchali, S. (2015). An Algorithm for Determining Kinetic Parameters of the Dissociation of Complex Solid Fuels. In print SAIMM.

Milani, L., Kinnaird, J.A., Lehmann, J., Naydenov, K. V., Saalmann, K., Frei, D., Gerdes, A. 2015. Role of crustal contribution in the early stage of the Damara Orogen, Namibia: new constraints from combined U-Pb and Lu-Hf isotopes to the Goas Magmatic Complex, Gondwana Research, 28(3), 961-986, doi:10.1016/j.gr.2014.08.007.

Milani, L., Lehmann, J., Naydenov, K. V., Saalmann, K., Kinnaird, J. A., Frei, D., Daly, J. S., Lobo-Guerrero Sanz, A. 2015. Geochemistry and petrogenesis of the Hook Batholith, Central Zambia: A-type magmatism in a syn-collisional setting, Lithos, 216-217, 48-72, doi:10.1016/j.lithos.2014.11.029.

Mohr-Westheide, T., Reimold, W. U., Fritz, J., Koeberl, C., Salge, T., Hofmann, A., and Schmitt, R. T. (2015). Discovery of extraterrestrial component carrier phases in Archean spherule layers: Implications for estimation of Archean bolide sizes. Geology 43, 299–302.

Montinaro, A., Strauss, H., Mason, P.R.D., Roerdink,D., Muenker, C., Schwarz-Schampera, U., Arndt, N.T., Farquhar, J., Beukes, N.J., Gutzmer, J. and Peters, M., 2015. Paleoarchean sulfur cycling; multiple sulfur isotope constraints from the Barberton greenstone belt, South Africa. Precambrian Research, 267: 311-322

Naydenov, K.V., Lehmann, J., Saalmann K., Milani, L,. Poterai, J., Kinnaird, J. A., Charlesworth, G., Kramers, J.D., 2015. The geology of the Matala Dome: an important piece of the Pan-African puzzle in Central Zambia. International Journal of Earth Sciences, doi: 10.1007/s00531-015-1222-y

Ndlalose, M., Malumbazo N., Wagner, N.J. (2015) Coal quality and uranium detection in Springbok Flats Coalfield samples. In print. SAIMM.

Perritt, S., Preston, R., Viljoen, F., van der Linde, G. (2015) Morphology, micro-structure and chemistry of a deformed garnet megacryst suite. South African Journal of Geology 118.4 : 439-454.

Pienaar, D., Guy, B. M., Hofmann, A. and Viljoen, K. S. (2015). A Geometallurgical Characterization of the Vaal Reef A-Facies at the Moab Khotsong Mine, Klerksdorp Goldfield, South Africa. South African Journal of Geology 118, 455-472.

Reinhardt, J., Elburg, M.A., Andersen, T. (2015). Zircon U-Pb age data and Hf isotope signature of Kaapvaal basement granites from the Archaean White Mfolozi Inlier, northern KwaZulu-Natal. South African Journal of Geology 118, 473-488.

Ruppel, A., Laeufer, A., Jacobs, J., Elburg, M., Krohne, N., Damaske, D., Lisker F. (2015). The Main Shear Zone in Sør Rondane, East Antarctica: Implications for the late-Pan-African tectonic evolution of Dronning Maud Land. Tectonics 34, 1290-1305.

Satkoski, A.M., Beukes,N.J., Li, W., Beard, B.L. and Johnson, C.M., 2015. A redox-stratified ocean 3.2 billion years ago. Earth and Planetary Science Letters, 430: 43-53

Simonson, B.M., Goderis, S. and Beukes, N.J., 2015. First detection of extraterrestrial material in ca. 2.49 Ga impact spherule layer in Kuruman Iron Formation, South Africa. Geology, 43: 251-254

Smith, A.J.B. (2015). The life and times of banded iron formations. Geology, 43, 1111-1112.

Van Wilderode, J., Debruyne, D., Torremans, K., Elburg, M., Vanhaecke, F., Muchez, Ph. (2015). Metal sources for the Nkana and Konkola stratiform Cu-Co deposits (Zambian Copperbelt): insights from Sr and Nd isotope ratios. Ore Geology Reviews 67, 127-138.

Viehmann, S., Bau, M., Smith, A.J.B., Beukes, N.J., Dantas, E.L. and Bühn, B. (2015). The reliability of ~2.9 Ga old Witwatersrand banded iron formations (South Africa) as archives for Mesoarchean seawater: Evidence from REE and Nd isotope systematics. Journal of African Earth Sciences, 111, 322-334.

Vorster, C., Kramers, J., Beukes, N., van Niekerk, H., 2015. Detrital zircon U–Pb ages of the Palaeozoic Natal Group and Msikaba Formation, Kwazulu-Natal, South Africa: provenance areas in context of Gondwana. Geological Magazine, doi:10.1017/S0016756815000370

Wohlgemuth-Ueberwasser CC, Viljoen F, Petersen S, Vorster C (2015) Distribution and solubility limits of trace elements in hydrothermal black smoker sulfides: An in-situ LA-ICP-MS study. Geochimica et Cosmochimica Acta 159 : 16-41.

PRESENTATIONS AT INTERNATIONAL CONFERENCES, with abstracts, 2015

Andersen, T., Elburg, M., Kristoffersen, M. (2015). How robust is the crustal evolution information from detrital zircon? Goldschmidt conference, August 2015, Prague.

Bons, P.D., Baur, A., Elburg, M.A., Lindhuber, M.J., Marks, M.A.W., Soesoo, A., van Milligen, B.P., Walte, N.P. (2015). Hindered settling and the formation of layered intrusions. EGU conference 2015, April 2015, Vienna

Cairncross, B. (2015). The Kalahari Manganese Field: Discovery, development and divine minerals. 6th Dallas Mineral Symposium, Dallas, Texas USA, 21-23 August. Invited keynote speaker.

Cairncross, B. and Bowell, R. (2015). Darkest copper: Classic and contemporary copper minerals of note from Africa. 6th Dallas Mineral Symposium, Dallas, Texas USA, 21-23 August. Invited keynote speakers.

Chitsiga T.L, Daramola, M.O., Wagner N.J., Ngoy, J.M. 2015. Effect of the presence of water-soluble amines on the Carbon Dioxide (CO2) adsorption capacity of amine-grafted poly-succinimide (PSI) adsorbent during CO2 Capture. TCCS-8, Trondheim, Norway, June 2015.

Delvigne, C., Opfergelt, S., Hofmann, A., Cardinal, D., & André, L. (2015). Si transfers during Archean weathering processes traced by silicon isotopes and Ge/Si ratios. In EGU General Assembly Conference Abstracts (Vol. 17, p. 4858).

Dongre A, Chalapathi Rao NV, Viljoen F (2015) Mineralogy and geochemistry of Timmasamudram kimberlites, southern India: Constraints on genesis and orangeite (Group II kimberlite) affinity of TK1 and TK4 pipes. Abstracts 13th Society for Geology Applied to Mineral Deposits (SGA) Biennial Meeting, 24-27 August 2015 Nancy, France (abstract 61421).

Dongre A, Jacob DE, Stern RA, Viljoen KS (2015) Eclogite xenoliths with subducted oceanic crust signatures from the Wajrakarur kimberlites, Southern India: Evidences from trace element and O isotope geochemistry. Abstracts Goldschmidt 2015, Prague, Czech Republic, 16 – 21 August 2015, p. 763.

Eickmann B, Hofmann A, Agangi A, Wille M., Meffre S, Wing B, Schoenberg R (2015). New insights into the 3.4 Ga sulphur and iron cycle from the ICDP Buck Reef Chert drill core.Goldschmidt 2015 Abstracts.

Elburg MA, Jele N, Andersen T, Watkeys M, Agangi A, Hofmann A (2015). Palaeoarchean intermediate – felsic volcanics of the Toggekry Formation, Nondweni Greenstone Belt, RSA: A rifted volcanic arc? Goldschmidt 2015 Abstracts.

Elburg, M., Andersen, T., Jacobs, J., Läufer, A., le Roux, P., Harris, C., Ruppel, A., Krohne, N., Damaske, N. (2015). Spatial and temporal influences on the geochemical signature of Pan-African magmatism in the Sør Rondane Mountains (East Antarctica). XII International Symposium on Antarctic Earth Sciences, July 2015, Goa, India.

Elburg, M.A., Jele, N., Andersen, T., Watkeys, M., Agangi, A., Hofmann, A. (2015). Palaeoarchean intermediate - felsic volcanics of the Toggekry Formation, Nondweni Greenstone Belt, RSA: a rifted volcanic arc? Goldschmidt conference, August 2015, Prague.

Hofmann A (2015). Greenstone belts as archives of early Earth processes.Goldschmidt 2015 Abstracts.

J.M. Ngoy, O. Bolland, N. Wagner, L. Riboldi, H. Potgieter "Influence of Moisture on Multi-Walled Carbon Nanotube with Polyaspartamide for CO2 Capture. 8th Trondheim Conference on CO2 Capture, Transport and Storage (TCCS-8), Trondheim, Norway June 16-18, 2015.

Jacobs, J., Elburg, M., Laeufer, A., Kleinhanns, I.C., Henjes-Kunst, F., Estrada, S., Ruppel, A., Damaske, D. (2015). The Geology and Geochronology of a Tonian Oceanic Arc Super Terrane (TOAST) in Eastern Dronning Maud Land. XII International Symposium on Antarctic Earth Sciences, July 2015, Goa, India.

Keren Osler, Michael O. Daramola, Dhruti Dheda, Jacob Ngoy, Nicola Wagner. Comparative Study of CO2 Adsorption Capacity of Single-walled and Multi-walled Carbon Nanotubes. 8th Trondheim Conference on CO2 Capture, Transport and Storage (TCCS-8), Trondheim, Norway June 16-18, 2015

Koeberl C, Schulz T, Özdemir S, Mohr-Westheide T, Reimold W U, and Hofmann A (2015). Remnants of early Archean impact events on Earth: new studies on spherule layers from the Barberton Mountain Land, South Africa. Workshop on Early Solar System Impact Bombardment III. LPI Contribution No. 1826, p.3017.

Laeufer, A., Jacobs, J., Elburg, M., Ruppel, A., Kleinhanns, I.C., Mieth., M., Jokat, W., Estrada, S., Henjes-Kunst, F., Egles, G. (2015). Geodynamic Evolution of Eastern Dronning Maud Land Based on Research Highlights from an International Geological-Geophysical Approach. XII International Symposium on Antarctic Earth Sciences, July 2015, Goa, India.

Mavhengere, P., Maphala, T., Wagner, N., 2015. Effects of Carbon Dioxide Storage on Vitrinite-Rich Coal Particles under Supercritical Conditions. -P-. 2015. International Conference on Coal Science & Technology , 27 Sept – 01 Oct 2015, Melbourne, Australia. Paper no. 3127379.

Mavhengere, P., Wagner, N., Kauchali, S., 2015. The Application of a Modified Distributed Activation Energy based Algorithm to Combustion and Gasification of Biomass-Coal Char Blends.-. The 7th International Conference on Clean Coal Technologies, 17 – 21 May 2015, Krakow, Poland

Mohr-Westheide, T., Reimold, W.U., Greshake, A., Hoehnel, D., Fritz, J., Schmitt, R.T., Salge, T., Hofmann, A., Oezdemir, S., Schulz, T. and Koeberl, C., 2015, July. PGE Chemistry and Systematics of Some Archean Spherule Layers in the Barberton Mountain Land. In 78th Annual Meeting of the Meteoritical Society (Vol. 1856, p. 5060).

Mohr-Westheide, T.; Fritz, J.; Reimold, W. U.; Koeberl, C.; Salge, T.; Hofmann, A.; Luais, B.; Hoehnel, D.; Özdemir, S.; Mader, D. (2015) Discovery of Extraterrestrial Component Carrier Phases in Archean Spherule Layers from the Barberton Greenstone Belt, South Africa. 46th Lunar and Planetary Science Conference. LPI Contribution No. 1832, p.1864.

Nxumalo, V., Kramers, J., Vorster, C. and Cairncross, B. (2015). Uranium in the coal zones of the Springbok Flats Basin, South Africa. Abstract. 31st International Association of Sedimentologists (IAS) Meeting of Sedimentology, Kraków, Poland 22-25 June 2015, p. 384.

Nxumalo, V., Kramers, J., Vorster, C. and Cairncross, B. (2015). Uranium mineralisation in the Springbok Flats Basin, South Africa. Abstract. Society for Geology Applied to Mineral Deposits (SGA), 13th Biennial Meeting, Nancy France, 24-27 August 2015.

Nxumalo, V., Kramers, J., Vorster, C., Cairncross, B., 2015. Uranium Mineralisation in the Springbok Flats Basin, South Africa. Proceeding of the 13th Biennial SGA Meeting, 24-27 August 2015, Nancy, France, pp 1859-1862.

Özdemir S, Koeberl C, Schulz T, Reimold WU, Mohr-Westheide T, Hofmann A (2015). A view to the first half of the Earth's impact history: Barberton CT3 spherule layers, South Africa. Goldschmidt 2015 Abstracts.

Özdemir, S., Koeberl, C., Schulz, T., Reimold, W. U., & Hofmann, A. (2015). Early terrestrial impact events: Archean spherule layers in the Barberton Greenstone Belt, South Africa. In EGU General Assembly Conference Abstracts (Vol. 17, p. 11076).

Premlall, K and Wagner, N.J., LABORATORY EXPERIMENTS TO DETERMINE BEST POTENTIAL FOR CYCLIC SUPERCRITICAL CO2 INJECTION IN SA COALS TO EVALUATE CH4 DESORPTION FOR ECBM POTENTIAL, International Conference on Coal science and Technology (ICCS&T), 27th – 30th September 2015, Melbourne Convention & Exhibition Centre, Melbourne, Australia.

Rose D, Viljoen F, Mouri H, Mulaba A (2015) Geometallurgical characterisation of Merensky Reef and UG2 at the Two Rivers platinum mine, Eastern Bushveld Complex, South Africa. Abstracts 12th International Congress for Applied Mineralogy, Istanbul, Turkey, 10-12 August 2015, Istanbul Technical University, p. 52.

Ruppel, A., Laeufer, A., Jacobs, J., Elburg, M., Krohne, N., Eagle, G., Mieth, M., Damaske, D., Lisker F. (2015). Pan-African Strike-Slip Tectonics in the Sør Rondane Region, Dronning Maud Land, and Lateral Extrusion of the East African-Antarctic Orogen. XII International Symposium on Antarctic Earth Sciences, July 2015, Goa, India.

PRESENTATIONS AT LOCAL CONFERENCES, PUBLIC LECTURES, REPORTS, 2015

Andersen, T., Elburg M. (2015). Zirconium in pyroxene: controlling factors and implications. IMSG conference, Pretoria, January 2015.

Cairncross, B. (2015). Geology as Art: a geological photographic perspective. Faculty of Science Public Lecture, University of Johannesburg 8th October 2015. INVITED LECTURE.

Cairncross, B. (2015). Pegmatites of Central Namibia: Geology, minerals and gemstones. Witwatersrand Gem & Mineral Club, 27th May 2015. INVITED SPEAKER.

Cairncross, B. (2015). The Kalahari Manganese Field: Discovery, development and divine minerals. Witwatersrand Gem & Mineral Club, 30th September 2015. INVITED SPEAKER.

Cairncross, B. and Fraser, A. (2015). Evaluation of the Council for Geoscience collection on public display in Ditsong Museum and in storage at the CGS offices, Silverton, Pretoria. *Unpublished confidential report plus appendices, Council for Geoscience, Pretoria*, 27 pages.

Elburg, M.A., Andersen, T., Jacobs, J., Läufer, A., le Roux, P., Tinguely, C., Janney, P.E., Ruppel, A., Krohne, N., Damaske, D. (2015). Pan-African magmatism in Sør Rondane (East Antarctica): 150 Ma of crustal recycling? IMSG conference, Pretoria, January 2015.

Hlongwane, S., Mphaphuli, M., Sebola M—J., Drennan, G. 2015. Structural and weathering effects on coal quality in the Soutpansberg and Tuli coalfields. Limpopo Minerals Conference and Trade Show. 10-12 November 2015, Park Hotel, Mokopane, Limpopo, South Africa.

Matiane, A., Wagner, N. 2015. Consideration of rare earth elements associated with coal and coal ash in South Africa. Fossil Fuel Foundation 20th South African Conference on research in Coal Science and Technology, 24 – 25 November, 2015, Potchefstroom, South Africa

Mphaphuli, M., Wagner, N. 2015. Petrographic consideration of the impact of the Tshipise fault on coal quality in the Soutpansberg coalfield. Fossil Fuel Foundation 20th South African Conference on research in Coal Science and Technology, 24 – 25 November, 2015, Potchefstroom, South Africa

Nendouvhada, N., Wagner, N. 2015. Lateral comparison of coal composition in the Botswana coalfields through the use of coal petrography. Fossil Fuel Foundation 20th South African Conference on research in Coal Science and Technology, 24 – 25 November, 2015, Potchefstroom, South Africa.

Premlall, K and Wagner, N.J., 2015. LABORATORY EXPERIMENTS TO DETERMINE THE FEASIBILITY OF CYCLIC CO2 INJECTION IN SA COALS TO EVALUATE CH4 DESORPTION FOR ECBM POTENTIAL, 3rd African Public Officials Energy and Environment Conference (APOEEC) HOST(S): Centre for Energy and Electric Power (Tshwane University of Technology Station); Tshwane Municipality and ESKOM, South Africa, 3-5th June 2015, Saint George Hotel and Convention Centre, Pretoria, South Africa.

SUPPORT STAFF IN PPM AND GEOLOGY

Lisborn Mangwane and Baldwin Tshivhiahuvhi: Technical assistants, thin section laboratory.

Daniel Selepe: Technical assistant, field vehicle maintenance.

Thuso Ramaliba: Laboratory Assistant, thin section laboratory.

Herbert Gugwane: Technical assistant, rock preparation laboratory.

Diana Khoza: Finance and transport.

Hennie Jonker: Finance and field schools.

Herbert Leteane: Technical assistant.

Elaine Minnaar: Departmental Secretary.

PPM ANNUAL RESEARCH COLLOQUIUM

Date: Thursday, 27 October 2016

Place: University of Johannesburg, Kingsway Campus, C1 Lab lecture room 215

Programme of talks also to be announced closer to the date

Time: 13.00 – 18.00, followed by drinks and snacks

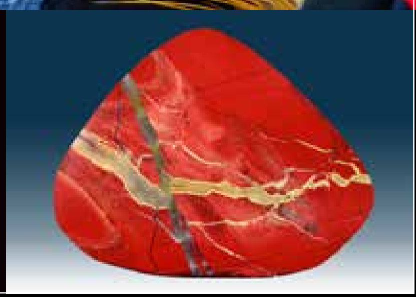

SPECTRUM

SPECTRUM, the Central Analytical Facility of the Faculty of Science at UJ, was established in 1999 to serve as a one-stop state-of-the-art unit, managed and staffed to ensure an accessible analytical service not only for UJ staff and students but also for outside cooperation and clients.

SPECTRUM offers comprehensive solutions for a broad range of applications, utilizing modern high-technology equipment. This includes PANalytical X'Pert Pro X ray diffraction (XRD) and Magix Pro X ray fluorescence (XRF) instruments, a Tescan Vega3 scanning electron microscope (SEM) with EDX detector for semiquantitative chemical analysis, a JEOL 733 microprobe, a Spectro ARCOS ICP optical emission spectrometer (OES), a Perkin Elmer NexION 350 ICP quadrupole mass spectrometer (ICP-QMS) for solution analysis, a Varian Unity Inova NMR system, and Zeiss Axioplan 2 compound and Zeiss Discovery stereo microscopes.


Argon extraction and mass spectrometer

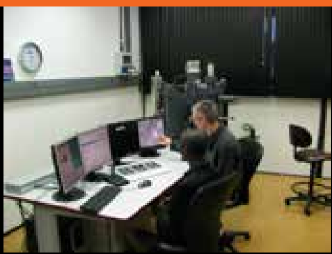
Electron microprobe


Laser ablation ICP-MS


Laser ablation multicollector ICP-MS

SPECIALIZED GEOSCIENCE APPLICATIONS AT SPECTRUM

Other than the more general instrumentation at SPECTRUM mentioned above, the facility also houses five units (two of them unique in Africa) geared specifically to Geoscience applications, among them the needs of PPM:

- A FEI Quanta 600F field emission Mineral Liberation Analyzer (MLA). This instrument is the one mainly used in geometallurgical research.
- A CAMECA SX100 electron microprobe with 4 wavelength dispersive spectrometers (WDS) and an energy dispersive spectrometer (EDS), used extensively for in situ micrometer-scale quantitative chemical analysis of minerals in a broad spectrum of projects.
- A ThermoFischer X-Series II ICP quadrupole mass spectrometer coupled to a New Wave UP-213 Nd YAG laser ablation system, as well as a Nu Instruments Nu Plasma II multicollector ICP mass spectrometer, coupled to a Resolution 199 nm excimer laser ablation system, are dedicated to *in situ* isotope and chemical analysis of minerals on a microscopic scale. The quadrupole system is particularly suited to rapid series of uranium-lead zircon age determinations, for instance in sediments, and trace element geochemical profiling. The multicollector system enables high-precision uranium-lead dating of zircon and other uranium-bearing minerals, as well as high precision isotope ratio analyses on strontium, neodymium, hafnium and many other elements, from both laser ablation and samples in solution.
- A MAP-215 noble gas mass spectrometer coupled to an ultra-high vacuum gas extraction system using a continuous 1064 nm Nd-YAG laser as a heat source. This is the only functional unit of its kind in Africa and is chiefly used for both $^{40}Ar/^{39}Ar$ and (in conjunction with the solution ICP-QMS system) U-Th-He geochronology.
- A paleomagnetic laboratory, likewise unique in Africa. This is equipped with a SQUID magnetometer and a fully automated snake chain sampling system, allowing for rapid and accurate measurements of samples for paleomagnetic studies.

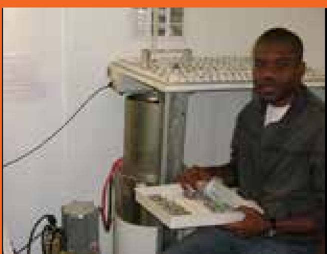
SQUID magnetometer with sample magazine


Solution ICP-MS


X ray diffraction


X ray fluorescence

For further information and cost of services please contact: Dr Willie Oldewage, Tel: 011 559 2274; Fax: 011 559 3361; e-mail: willieho@uj.ac.za